Applied Energy 237 (2019) 241–257

Contents lists available at ScienceDirect

Applied Energy

journal homepage: www.elsevier.com/locate/apenergy

A performance-guided JAYA algorithm for parameters identification of photovoltaic cell and module

Kunjie Yu[a], Boyang Qu[b], Caitong Yue[a], Shilei Ge[a], Xu Chen[c], Jing Liang[a,*]

[a] School of Electrical Engineering, Zhengzhou University, Zhengzhou 450001, China
[b] School of Electric and Information Engineering, Zhongyuan University of Technology, Zhengzhou 450007, China
[c] School of Electrical and Information Engineering, Jiangsu University, Zhenjiang 212013, China

HIGHLIGHTS

- PGJAYA is proposed to estimate the model parameters of PV cell and module.
- Individual performance is quantified to assign update strategy to individual.
- Self-adaptive chaotic perturbation is used to improve the population quality.
- Experimental results indicate the superior performance of PGJAYA.

ARTICLE INFO

Keywords:
Parameters identification
Photovoltaic cell and module
JAYA algorithm
Optimization

ABSTRACT

In order to carry out the evaluation, control and maximum power point tracking on photovoltaic (PV) systems, accurate and reliable model parameter identification of PV cell and module is always desired. In this study, a performance-guided JAYA (PGJAYA) algorithm is proposed for extracting parameters of different PV models. In proposed PGJAYA algorithm, the individual performance in the whole population is quantified through probability. Then, based on probability, each individual can self-adaptively select different evolution strategies designed for balancing exploration and exploitation abilities to conduct the searching process. Meanwhile, the quantified performance is employed to select the exemplar to construct the promising searching direction. In addition, a self-adaptive chaotic perturbation mechanism is introduced around the current best solution to explore more better solution for replacing the worst one, thus improving the quality of whole population. The parameters estimation performance of PGJAYA is evaluated through three widely used standard datasets of different PV models including single diode, double diode, and PV module. Comparative and statistical results demonstrate that PGJAYA has a superior performance as it always obtains the most accurate parameters with strong robustness among all compared algorithms. Furthermore, the tests based on experimental data from the data sheet of different types of PV modules suggest that the proposed algorithm can achieve superior results at different irradiance and temperature. Based on these superiorities, it is concluded that PGJAYA is a promising parameter identification method for PV cell and module model.

1. Introduction

In recent years, to cope with the environment pollution, climate change, and increasing energy shortage, many efforts have been focused on the research of renewable energy [1,2]. Among the various available sources of renewable energy, the solar photovoltaic (PV) cell based energy sources is the most potential and promising alternative [3,4]. With the development of PV technology, accurate modeling and parameter estimation that can closely represent the nonlinear current-voltage characteristics of solar cells have drawn considerable attention in evaluation, control, and maximum power point tracking of PV systems [5,6]. Although many mathematic models have been proposed to describe the nonlinear behavior of PV systems, two parameter equivalent circuit models namely single diode model and double diode model are commonly employed in practice [7]. The accuracy of these models is mainly determined by their model parameters, but these parameters are often unavailable and varying since the faults, aging, and changed operation conditions [8]. As a consequence, an accurate knowledge of

* Corresponding author.
E-mail address: liangjing@zzu.edu.cn (J. Liang).

https://doi.org/10.1016/j.apenergy.2019.01.008
Received 29 August 2018; Received in revised form 11 December 2018; Accepted 1 January 2019
Available online 08 January 2019

these parameters is vital to the performance evaluation, quality control, and maximum power point tracking of PV systems. However, the implicit transcendental equations of single diode model and double diode model challenge the common elementary functions [9]. Hence, it is expected and important to design efficient and reliable technique to identify these model parameters based on the measured current-voltage data of PV cell and module.

The problem of extracting the PV cell and module models parameters can be converted into an optimization problem, and an objective function need to be defined. A certain degree of noise in the measured current-voltage data results into the search space is nonlinear and multimodal containing multiple local optimal [10], which brings about challenges for the designing of one parameter estimation method [11]. Generally, there are two classes of methods namely deterministic method and heuristic method in estimating the PV models parameters. When using deterministic techniques, a number of model restrictions such as differentiability and convexity are required. In addition, the performance of deterministic technique is significantly affected by its initial solution [12]. As a result, the results obtained by deterministic methods are unsatisfied and uncertain. In contrast, heuristic algorithms feature some obvious advantages such as imposing no restrictions on the problem formulation, conceptual and computational simplicity, and being excellent for multimodal problems [13,14]. Therefore, many heuristic methods have been employed and improved to identify the PV models parameters in the past decade. They are particle swarm optimization [15,16], genetic algorithm [17], differential evolution [18], artificial bee colony [19,20], teaching-learning-based optimization [10,21], harmony search [22], ant lion optimizer [23], biogeography-based optimization [12], flower pollination algorithm [24–26], whale optimization algorithm [27], JAYA algorithm [28], and other algorithms [29–31]. Compared with deterministic methods, although these heuristic methods have provided more robust and accurate results, it is still difficult to find the global optimal for most of heuristic algorithms. The main reason is that the PV models parameters estimation is a multimodal problem with a lot of local optima. Moreover, in addition to two common parameters namely the population size and the number of generation, many heuristic methods have their own algorithm-specific control parameters and their performance strongly depends on the choice of algorithm-specific control parameters. Any improper tuning not only increases the computational burden but also results in premature termination. Hence, developing for a competitive heuristic algorithm to estimate the PV models parameters is still a challenging task.

Recently, a new and effective heuristic method named JAYA was proposed by Rao [32] for solving different kinds of optimization problems. In addition to two common algorithm parameters, JAYA requires no any algorithm-specific parameter. Thus, an obvious benefit of JAYA can be obtained in terms of omitting the difficulty of tuning parameters and reducing the time necessary for implementing optimization process. Due to its flexibility and efficiency, JAYA and its many variants have been used to deal with various optimization problems, such as optimization of wind farm layout [33], job-shop rescheduling [34], battery model parameter estimation [35], PV system maximum power point tracking [36], thermal devices design [37], economic load dispatch [38], heat exchangers [39], optimum power flow problem [40,41], and other real-world problems [42,43]. In [28], an improved JAYA (IJAYA) algorithm was developed to deal with the parameters estimation problems of PV models, and satisfied results were obtained. However, the solution in IJAYA is updated through two strategies totally randomly without considering the solution performance in population, leading to the difficult to achieve the appropriate balance between exploration and exploitation abilities. Furthermore, although the chaotic elite learning method was used in IJAYA to refine the quality of the best solution in each generation, it ignored the fact that different perturbations around the best solution should be allocated to different searching stages. As a result, the performance improvement of IJAYA is limited and need to be further enhanced when solving the parameters estimation problems of PV models.

Based on the above considerations, in this paper, a performance-guided JAYA (PGJAYA) algorithm is proposed to extract the parameters of PV cell and module models more accurately and reliably. To be specific, the individual performance in population of PGJAYA is quantified through ranking, and then one probability is assigned to each individual to represent its performance in current population. Based on the probability, each individual can self-adaptively select a proper evolution strategy to specially enhance the corresponding searching ability. In this way, the computational resource is assigned reasonably, and thus the balancing between exploration and exploitation abilities would be achieved. This performance-guided process is self-adaptive and could be more effective than the totally random process employed in IJAYA. In addition, compared with the chaotic elite learning method in IJAYA, the chaotic searching of PGJAYA is employed around the current best solution with different disturbances at different searching stages, to obtain more better solution for replacing the worst one, thus improving the quality of whole population. In order to evaluate the effectiveness of the proposed PGJAYA algorithm, it is first compared with other state-of-the-art algorithms on three parameters identification problems of PV cell and module, and then tested on three PV modules of different types at different irradiance and temperature. Extensive experimental results and analyses indicate that PGJAYA can obtain more accurate and reliable results with competitive computation efficiency than all compared algorithms.

The main contributions of this study are summarized as follows:

- A novel method PGJAYA is developed to estimate the parameters of PV cell and module models. Based on quantified performance, individual can self-adaptively select the proper update strategy to promote the related searching ability.
- The quantified performance is also used to select the exemplar to construct the promising searching direction.
- A self-adaptive chaotic perturbation mechanism is employed around the current best solution to explore more better solution for replacing the worst one.
- Comprehensive experiments are designed and carried out to evaluate the effectiveness of PGJAYA.

The remainder of this paper is organized as follows. Section 2 gives the mathematical model of PV cell and module. Section 3 brief introduces the JAYA algorithm. Section 4 provides the proposed PGJAYA in detail. Section 5 designs and shows the experimental results and analysis. Finally, the conclusions are presented in Section 6.

2. Photovoltaic modeling and problem formulation

As mentioned above, there are several mathematic models to describe the current-voltage characteristics of PV cell and module in the literature. Among them, the single diode model and double diode model are the most widely used in practice. Brief mathematical descriptions and problem formulation are presented below for these models.

2.1. Photovoltaic cell model

2.1.1. Single diode model

Fig. 1(a) provides the equivalent circuit diagram for single diode model [28]. It can be seen that the solar cell under illumination is modeled as a current source, a diode, and two resistors. The shunt resistor represents the leakage current, and the series resistor denotes the resistance in the path of the current including electrode resistance, contact resistance, and material bulk resistance. According to Kirchhoff's current law, the output current in Fig. 1(a) can be calculated by Eq. (1).

$$I_L = I_{ph} - I_d - I_{sh} \tag{1}$$

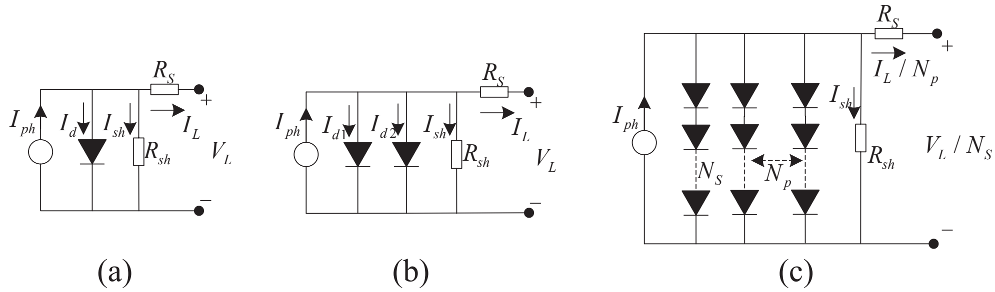

Fig. 1. Equivalent circuit model for (a) single diode, (b) double diode, and (c) PV module.

where I_L is the output current, I_{ph} is the photocurrent, I_d is the diode current, and I_{sh} is the shunt resistor current. According to Shockley diode equation, I_d can be calculated by Eq. (2).

$$I_d = I_{sd}\cdot\left[\exp\left(\frac{V_L + R_S\cdot I_L}{n\cdot V_t}\right) - 1\right] \tag{2}$$

where R_S is the series resistance, V_L is the output voltage, n is the diode ideality factor, I_{sd} is the reverse saturation current of diode, and V_t is the junction thermal voltage obtained by Eq. (3).

$$V_t = \frac{k\cdot T}{q} \tag{3}$$

where $k = 1.3806503 \times 10^{-23}$ J/K is the Boltzmann constant, T is the temperature in Kelvin, and $q = 1.60217646 \times 10^{-19}C$ is the electron charge.

The shunt resistor current I_{sh} can be calculated by Eq. (4).

$$I_{sh} = \frac{V_L + R_S\cdot I_L}{R_{sh}} \tag{4}$$

where R_{sh} is the shunt resistance.

Consequently, Eq. (5) can be obtained by combining Eqs. (1)–(4) to represent the relationship among the output current, output voltage, and model parameters.

$$I_L = I_{ph} - I_{sd}\cdot\left[\exp\left(\frac{q\cdot(V_L + R_S\cdot I_L)}{n\cdot k\cdot T}\right) - 1\right] - \frac{V_L + R_S\cdot I_L}{R_{sh}} \tag{5}$$

It can be seen from Eq. (5) that five unknown parameters (I_{ph}, I_{sd}, R_S, R_{sh}, n) need to be estimated in the single diode model. These parameters can be estimated by an optimization technique to reflect the solar cell performance, and high precision and robustness are desired.

2.1.2. Double diode model

Due to its simplicity and accuracy, the aforementioned single diode model has been widely employed to describe the static characteristic of solar cell. However, single diode model has inherent drawbacks as it assumes the diode ideality factor remains constant throughout the output voltage variation range [44]. In fact, diode ideality factor is a function of voltage across the device. Moreover, the effect of recombination current loss in the depletion region is neglected in single diode model. Considering all these issues and to make the model more realistic, as shown in Fig. 1(b), double diode model is obtained by adding a second recombination diode in parallel with the first diffusion diode. The output current of double diode model is calculated by Eq. (6).

$$\begin{aligned} I_L &= I_{ph} - I_{d1} - I_{d2} - I_{sh} \\ &= I_{ph} - I_{sd1}\cdot\left[\exp\left(\frac{q\cdot(V_L + R_S\cdot I_L)}{n_1\cdot k\cdot T}\right) - 1\right] - I_{sd2}\cdot\left[\exp\left(\frac{q\cdot(V_L + R_S\cdot I_L)}{n_2\cdot k\cdot T}\right) - 1\right] \\ &\quad - \frac{V_L + R_S\cdot I_L}{R_{sh}} \end{aligned} \tag{6}$$

where I_{sd1} and I_{sd2} represent the diffusion and saturation currents, respectively. n_1 and n_2 represent the diffusion and recombination diode ideality factors, respectively. It can be observed from Eq. (6) that seven unknown parameters (I_{ph}, I_{sd1}, I_{sd2}, R_S, R_{sh}, n_1, n_2) should be extracted.

2.2. Photovoltaic module model

As presented in Fig. 1(c), the single diode PV module model is built by combining several solar cells connected in series and/or in parallel. The output current of single diode PV module can be calculated by Eq. (7).

$$I_L = N_p\cdot I_{ph} - N_p\cdot I_{sd}\cdot\left[\exp\left(\frac{q\cdot(V_L/N_S + R_S\cdot I_L/N_p)}{n\cdot k\cdot T}\right) - 1\right] - \frac{N_p\cdot V_L/N_S + R_S\cdot I_L}{R_{sh}} \tag{7}$$

where N_p is the number of solar cells in parallel, and N_S is the number of solar cells in series. It is clear that five unknown parameters (I_{ph}, I_{sd}, R_S, R_{sh}, n) need to be identified.

2.3. Problem formulation

The parameters identification of PV cell and module models is converted into an optimization problem by minimizing the difference between the experimental and calculated data. For each pair of experimental and calculated current data point, the error function can be obtained by Eqs. (8) and (9) for single diode model and double diode model, respectively.

$$\begin{cases} f_k(V_L, I_L, \mathbf{x}) = I_{ph} - I_{sd}\cdot\left[\exp\left(\frac{q\cdot(V_L + R_S\cdot I_L)}{n\cdot k\cdot T}\right) - 1\right] - \frac{V_L + R_S\cdot I_L}{R_{sh}} - I_L \\ \mathbf{x} = \{I_{ph}, I_{sd}, R_S, R_{Sh}, n\} \end{cases} \tag{8}$$

$$\begin{cases} f_k(V_L, I_L, \mathbf{x}) = I_{ph} - I_{sd1}\cdot\left[\exp\left(\frac{q\cdot(V_L + R_S\cdot I_L)}{n_1\cdot k\cdot T}\right) - 1\right] \\ \qquad - I_{sd2}\cdot\left[\exp\left(\frac{q\cdot(V_L + R_S\cdot I_L)}{n_2\cdot k\cdot T}\right) - 1\right] - \frac{V_L + R_S\cdot I_L}{R_{sh}} - I_L \\ \mathbf{x} = \{I_{ph}, I_{sd1}, I_{sd2}, R_S, R_{Sh}, n_1, n_2\} \end{cases} \tag{9}$$

Then, the overall difference is quantified by the root mean square error (RMSE) defined by Eq. (10) [10–12,21,25,45]. As a result, the parameters can be estimated by minimizing the objective function RMSE($\mathbf{x}$) by means of searching the solution vector $\mathbf{x}$ within the parameter feasible range.

$$\mathrm{RMSE}(\mathbf{x}) = \sqrt{\frac{1}{N}\sum_{k=1}^{N} f_k(V_L, I_L, \mathbf{x})^2} \tag{10}$$

where $\mathbf{x}$ is the decision variable, N is the number of measured data, V_L and I_L are the measured voltage and current, respectively.

3. JAYA algorithm

As a new population-based intelligence optimization algorithm, JAYA is developed to deal with unconstrained and constrained optimization problems primitively. In each generation of JAYA algorithm, one solution is optimized by approaching to the optimal solution and evading the inferior solution simultaneously [32]. Different from most other population-based algorithms, JAYA requires no algorithm-specific parameters need to be tuned to achieve the proper performance, this feature makes it has a potential applicability and efficiency [41,42].

For an objective function $f(\mathbf{x})$ with D dimensional variables ($j = 1, 2, ...,D$), let $x_{i,j}$ to be the value of the jth variable for the ith candidate solution, thus $\mathbf{x}_i = (x_{i,1}, x_{i,2}, ...,x_{i,D})$ represents the position of ith candidate solution. If a solution has the best $f(\mathbf{x})$ value in the current population, it is the best candidate solution and denoted as $\mathbf{x}_{best} = (x_{best,1}, x_{best,2}, ...,x_{best,D})$. On the contrary, one solution is the worst candidate solution and denoted as $\mathbf{x}_{worst} = (x_{worst,1}, x_{worst,2}, ...,x_{worst,D})$ if it has the worst $f(\mathbf{x})$ value in the current population. Based on the best and worst solutions, each solution $x_{i,j}$ is updated by Eq. (11). The updated solution is accepted if it gives a better function value.

$$x'_{i,j} = x_{i,j} + rand_1 \cdot (x_{best,j} - |x_{i,j}|) - rand_2 \cdot (x_{worst,j} - |x_{i,j}|) \tag{11}$$

where $x_{best,j}$ and $x_{worst,j}$ respectively represent the values of the jth variable for the best and worst solutions. $|x_{i,j}|$ denotes the absolute value of $x_{i,j}$ and $x'_{i,j}$ denotes the updated value of $x_{i,j}$. $rand_1$ and $rand_2$ are two uniformly distributed numbers randomly generated within [0, 1]. Therefore, the tendency of the solution attracted by the best solution is represented by term $rand_1 \cdot (x_{best,j} - |x_{i,j}|)$, and the tendency of the solution to escape the worst solution is indicated by term $- rand_2 \cdot (x_{worst,j} - |x_{i,j}|)$. That is, in the searching process of JAYA, one solution is optimized by getting close to the best solution and keeping away from the worst solution simultaneously.

4. Performance-guided JAYA algorithm (PGJAYA)

4.1. Motivations

In general, the optimization performance of one population-based algorithm is mainly determined by its exploration ability and exploitation ability during the evolution process [46]. To be specific, exploration is the ability of an algorithm to explore the search space and seeking for new or unknown regions, while exploitation is the ability to improve and refine the solutions by exploiting information derived from existing solutions [47]. How to balance these two abilities with fair computational resource is the key issue for designing an efficient algorithm. In the basic JAYA algorithm, the solution is updated only by means of the best solution and the worst solution simultaneously, although the convergence rate is promoted, the population diversity cannot be maintained efficiently, weakening the exploration ability. In recent years, many attempts have been made to improve the population diversity of JAYA by introducing other update strategies. However, these studies rarely use the individual performance to guide the designing of updating mechanism, leading to the performance improvement is limited. If the individual performance in current population can be reasonably utilized to assign different individuals to enhance different searching abilities, the balancing between exploration and exploitation abilities can be achieved efficiently with the help of feedback information. Hence, based on these considerations, we propose a performance-guided JAYA algorithm to further improve the performance of JAYA in identifying the model parameters of PV cell and module. To be specific, the individual performance in the whole population is quantified through probability. Based on its probability, each individual can self-adaptively select the corresponding evolution strategy designed for promoting exploration or exploitation ability. Also, the probability is used to build the promising searching direction. Besides, by considering different searching stages, the chaotic searching is self-adaptively employed around the current best solution to obtain more better solution for replacing the worst one, thus improving the quality of whole population. The core idea behind PGJAYA is elucidated as follows.

4.2. Individual performance quantification

First, individuals in the population are sorted in ascending order (from the best to the worst) based on the fitness value. Afterwards, a ranking value R_i is assigned to ith individual using Eq. (12). Based on the ranking value of each individual, one probability computed by Eq. (13) as the indicator to reflect the individual performance. It can be clearly observed that the individual with better fitness has a larger probability.

$$R_i = NP - i, \quad i = 1, 2, ...,NP \tag{12}$$

$$P_i = (R_i/NP)^2 \tag{13}$$

where NP is the population size.

4.3. Performance-guided evolution process

Based on the above calculated probability, each individual can self-adaptively choose the corresponding update strategy to promote different searching abilities. Please note that the better individual will be expected to focus on improving the exploration ability to search different regions. While the inferior individual will be expected to enhance the exploitation ability to converge toward the promising region located by better individual. In view of this, the performance-guided evolution process can be described in Algorithm 1. It can be observed that the better individual has larger probability and is more likely to select strategy II to enhance the exploration ability, while the inferior individual has smaller probability and tends to choose strategy I to improve the exploitation ability. Through this division of labor, the balancing between exploration ability and exploitation ability will be achieved reasonably.

Algorithm 1.. Performance-guided evolution process

1. Sort all individuals in population in ascending order according to their fitness
2. Compute the probability P_i for each individual
3. **For** $i = 1$ to NP **do**
4. **If** $rand > P_i$ **then**
5. Implement the strategy I to enhance the exploitation ability
6. **Else**
7. Implement the strategy II to enhance the exploration ability
8. **End if**
9. **End for**

Considering that strategy I is devoted to improving exploitation ability, as shown in Eq. (14), the modified update equation proposed in [28] is employed in this study. Compared with the basic update Eq. (11), the new equation can be more efficiently by introducing a self-adaptive weight shown in Eq. (15). The reason is that the potential region can be found at the early stage as the degree of approaching the best solution is relatively larger, while at the later stage, the refine search can be achieved in potential region since the degree of approaching the best solution and avoiding the worst solution are similar.

$$x'_{i,j} = x_{i,j} + rand_1 \cdot (x_{best,j} - |x_{i,j}|) - w \cdot rand_2 \cdot (x_{worst,j} - |x_{i,j}|) \tag{14}$$

$$w = \begin{cases} \left(\frac{f(\mathbf{x}_{best})}{f(\mathbf{x}_{worst})}\right)^2, & \text{if } f(\mathbf{x}_{worst}) \neq 0 \\ 1, & \text{otherwise} \end{cases} \tag{15}$$

where $f(\mathbf{x}_{best})$ and $f(\mathbf{x}_{worst})$ respectively represent the objective function values of the best solution and worst solution.

As mentioned above, strategy II is used to enhance the exploration ability, so the population diversity is expected to be maintained efficiently. In this study, other two individuals are selected from the population to determine the searching direction for guiding the current individual to explore different regions. Moreover, considering that more better individual has more information about the potential search direction and if this information can be utilized in determining the searching direction, the exploration ability can be improved more efficiently. Therefore, the probability computed above is also used to select the exemplar to build the promising searching direction. To be specific, as presented in Eq. (16), the exemplar $\mathbf{x}_l^{P_l}$ is selected by considering its probability P_l computed by Eq. (13) and another individual $\mathbf{x}_m^R$ is selected randomly.

$$x'_{i,j} = x_{i,j} + rand\cdot(x_{l,j}^{P_l} - x_{m,j}^R) \tag{16}$$

where $x_{l,j}^{P_l}$ and $x_{m,j}^R$ are the values of the jth variable for the l and m individuals ($l \neq m \neq i$), respectively. $rand$ is a number generated randomly within [0, 1].

4.4. Self-adaptive chaotic perturbation

In evolution process, as the population is used to save the better solutions found so far and its quality is very important to the searching performance. In this study, to further improve the population quality, a self-adaptive chaotic perturbation mechanism is introduced to find the better solution around the current best solution for replacing the worst one. Considering that the randomicity and ergodicity in chaotic sequence are very helpful to further enhance one solution quality by exploring new solution around it [10,12,48], so the logistic map shown in Eq. (17) is employed. Furthermore, at the early stage, more perturbations are desired to disturb the best individual to obtain the better individuals. While at the latter stage, more information from the best individual is expected to be inherited since the best individual is quite close to the global optimum. Thus, as shown in Eq. (18), the chaotic perturbation is controlled by function evaluations to generate a new individual $\mathbf{x}^*$ around the best individual. Then, the new individual is used to replace the worst one if it gives better function value. In this way, the quality of current population can be improved by the self-adaptive chaotic perturbation.

$$z_{k+1} = 4\cdot z_k\cdot(1 - z_k) \tag{17}$$

$$x_j^* = \begin{cases} x_{best,j} + rand\cdot(2\cdot z_k - 1), & \text{if } rand < 1 - (FES/FES_{\max}) \\ x_{best,j}, & \text{otherwise} \end{cases} \tag{18}$$

where z_k is the value of kth chaotic iteration, and its initial value z_0 is randomly generated within [0, 1]. FES denotes the current number of function evaluations, and $FES_{\max}$ represents the maximum number of function evaluations.

4.5. Framework of PGJAYA

According to the aforementioned descriptions, Algorithm 2 gives the pseudo code of PGJAYA and Fig. 2 provides the flow chart. Compared with basic JAYA, PGJAYA also has a simple structure and requires no any additional parameter needs to be tuned. So PGJAYA is also free from algorithm-specific parameter.

For the computational complexity, compared with the original JAYA, the additional complexity of the proposed PGJAYA derives from the individual performance quantification process (i.e., population sorting and probability computation) and the self-adaptive chaotic perturbation. The complexity of population sorting is $O(NP\cdot\log(NP))$, the complexity of probability computation is $O(NP)$, and $O(D)$ is consumed to implement the self-adaptive chaotic perturbation. Since the complexity of basic JAYA is $O(G_{\max}\cdot NP\cdot D)$, where $G_{\max}$ is the maximal number of generation, the total complexity of PGJAYA is $O(G_{\max}\cdot(NP\cdot D + NP\cdot\log(NP) + NP + D))$. In general, the population size NP is set to be proportional to the problem dimension D. Hence, according to the complexity computation rules, the total complexity of PGJAYA is $O(G_{\max}\cdot NP\cdot D)$, which is the same as the original JAYA algorithm. Furthermore, the computational efficiency of PGJAYA is investigated in the following Section 5.1.

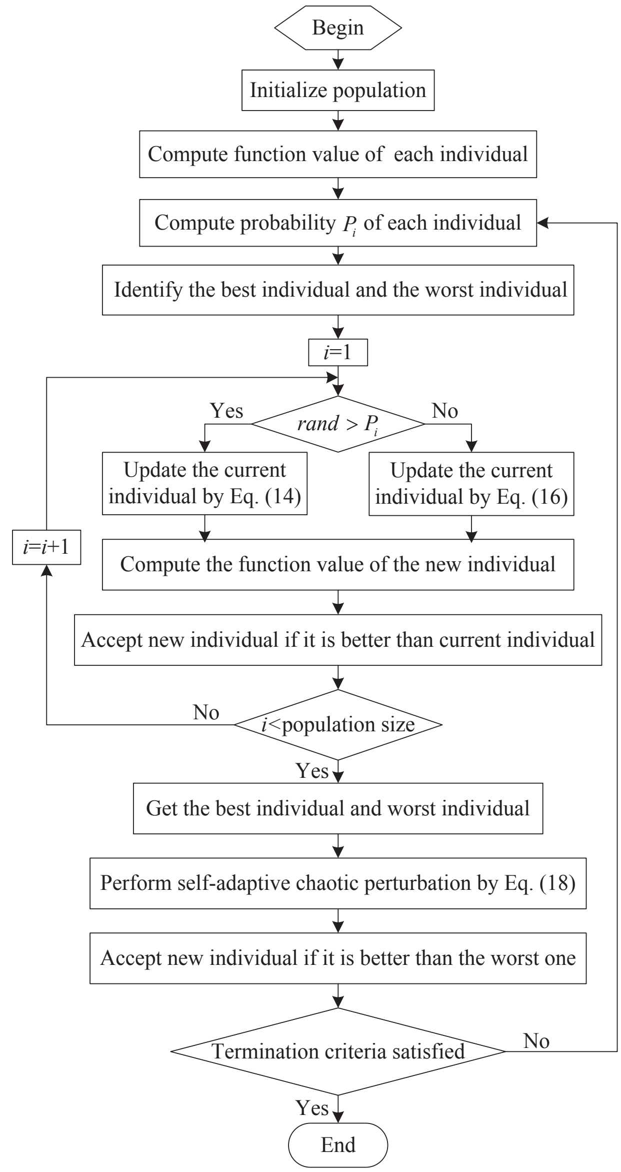

Fig. 2. The flow diagram of PGJAYA.

Table 1
Parameters ranges of RTC France PV cell and Photo Watt-PWP 201 PV module.

Parameter	Single diode/Double diode		PV module	
	Lower bound	Upper bound	Lower bound	Upper bound
I_{ph}(A)	0	1	0	2
I_{sd}, I_{sd1}, I_{sd2}(μA)	0	1	0	50
R_S(Ω)	0	0.5	0	2
R_{sh}(Ω)	0	100	0	2000
n, n_1, n_2	1	2	1	50

Table 2
Parameter settings of the compared algorithms.

Algorithm	Parameters
PGJAYA	$NP = 20$.
IJAYA	$NP = 20$.
JAYA	$NP = 20$.
GOTLBO	$NP = 50$, jumping rate $Jr = 0.3$.
STLBO	$NP = 20$.
TLABC	$NP = 50$, limit $= 200$, $F = rand$.
CLPSO	$NP = 40$, inertia weight w: 0.9–0.2, acceleration coefficient c = 1.49445, refreshing gap $m = 5$.
BLPSO	$NP = 40$, inertia weight w: 0.9–0.2, acceleration coefficient c = 1.49445, $I = E = 1$.
DE/BBO	$NP = 100$, $I = E = 1$, $\pi_{\max} = 0.005$, $K = 2$, $F = \text{rand}(0.1,1)$, $CR = 0.9$.
CMM-DE/BBO	$NP = 100$, $I = E = 1$, $\pi_{\max} = 0.005$, $K = 2$, $F = \text{rand}(0.1,1)$, $CR = 0.9$, $P_e = 0.5$.

Algorithm 2.. Pseudo code of PGJAYA

1. Initialize the population size NP and the maximum number of function evaluations $FES_{\max}$;
2. Generate the initial population randomly and evaluate the objective function value of each individual;
3. $FES = NP$;
4. **While** $FES < FES_{\max}$ **do**
5. Compute the probability P_i for each individual $\mathbf{x}_i$;
6. Identify the best individual and worst individual in current population;
7. **For** $i = 1$ to NP **do**
8. **If** $rand > P_i$ **then**
9. Implement the strategy I to update $\mathbf{x}_i$ by using Eq. (14);
10. **Else**
11. Randomly select $l \in \{1, NP\}$; %%The selection of exemplar $\mathbf{x}_l^{P_l}$
12. **While** $rand > P_l$ **or** $l = = i$ **do** Randomly select $l \in \{1, NP\}$ **End while**
13. Randomly select $m \in \{1, NP\}$; %%The selection of exemplar $\mathbf{x}_m^R$
14. **While** $m = = i$ **or** $m = = l$ **do** Randomly select $m \in \{1, NP\}$ **End while**
15. Implement the strategy II to update $\mathbf{x}_i$ by using Eq. (16);
16. **End if**
17. Compute the function value of the updated individual $\mathbf{x}_i'$;
18. $FES = FES + 1$;
19. Accept the new individual $\mathbf{x}_i'$ if it is better than the old one;
20. **End for**
21. Find the best individual and the worst individual in current population;
22. Perform the self-adaptive chaotic perturbation using Eq. (18) to generate a new individual $\mathbf{x}^*$;
23. Compute the function value of the new individual $\mathbf{x}^*$;
24. $FES = FES + 1$;
25. Accept the new individual $\mathbf{x}^*$ if it is better than the worst individual;
26. **End while**

5. Experimental results and discussions

In order to verify the effectiveness of the proposed PGJAYA, it is first used to solve parameters identification problems of PV cell and module models, including single diode model, double diode model, and PV module model. The experimental current-voltage data from [49] are selected as the benchmark data, which have been widely used to test various techniques designed for parameters estimation of PV models. These data are measured from a commercial silicon PV cell (RTC France) with 57 mm diameter at 33 °C under 1000 W/m^2 irradiance, and a PV module (Photo Watt-PWP 201) contains 36 polycrystalline PV cells in series at 45 °C under 1000 W/m^2 irradiance. In order to ensure that the searching space of each problem is the same, the ranges for each parameter are kept the same as those used in previous literatures. Table 1 provides the ranges for each parameter of PV cell and module models.

To validate the superior performance of PGJAYA, other nine well-established algorithms are selected to compare. They are the improved

Table 3
The statistical results for RTC France PV cell and Photo Watt-PWP 201 PV module.

Model	Algorithm	RMSE				Significance
		Min	Mean	Max	SD	
Single diode model of RTC France	PGJAYA	**9.8602E−04**	**9.8602E−04**	**9.8603E−04**	**1.4485E−09**	
	IJAYA	9.8603E−04	9.9204E−04	1.0622E−03	1.4033E−05	+
	JAYA	9.8946E−04	1.1617E−03	1.4783E−03	1.8796E−04	+
	GOTLBO	9.8856E−04	1.0450E−03	1.2067E−03	5.0218E−05	+
	STLBO	**9.8602E−04**	9.8607E−04	9.8655E−04	1.8602E−05	+
	TLABC	**9.8602E−04**	9.9417E−04	1.0308E−03	1.1896E−05	+
	CLPSO	9.9633E−04	1.0581E−03	1.3196E−03	7.4854E−05	+
	BLPSO	1.0272E−03	1.3139E−03	1.7928E−03	2.1166E−04	+
	DE/BBO	9.9922E−04	1.2948E−03	2.2258E−03	2.5074E−04	+
	CMM-DE/BBO	9.8605E−04	1.0486E−03	1.3475E−03	8.1679E−05	+
Double diode model of RTC France	PGJAYA	9.8263E−04	**9.8582E−04**	**9.9499E−04**	**2.5375E−06**	
	IJAYA	9.8293E−04	1.0269E−03	1.4055E−03	9.8325E−05	+
	JAYA	9.8934E−04	1.1767E−03	1.4793E−03	1.9356E−04	+
	GOTLBO	9.8742E−04	1.1475E−03	1.3947E−03	1.1330E−04	+
	STLBO	**9.8252E−04**	1.0585E−03	2.4480E−03	2.8978E−04	+
	TLABC	1.0012E−03	1.2116E−03	1.9826E−03	2.1100E−04	+
	CLPSO	9.9894E−04	1.1458E−03	1.5494E−03	1.4367E−04	+
	BLPSO	1.0628E−03	1.4821E−03	1.7411E−03	1.7789E−04	+
	DE/BBO	1.0255E−03	1.5571E−03	2.4042E−03	3.6297E−04	+
	CMM-DE/BBO	1.0088E−03	1.5487E−03	2.0589E−03	2.9413E−04	+
PV module model of Photo Watt-PWP 201	PGJAYA	**2.425075E−03**	**2.425144E−03**	**2.426764E−03**	**3.071420E−07**	
	IJAYA	2.425129E−03	2.428855E−03	2.439269E−03	3.775523E−06	+
	JAYA	2.427785E−03	2.453710E−03	2.595873E−03	3.456290E−05	+
	GOTLBO	2.426583E−03	2.475386E−03	2.563849E−03	2.938836E−05	+
	STLBO	**2.425075E−03**	2.055293E−02	2.742508E−01	6.896273E−02	+
	TLABC	**2.425075E−03**	2.425464E−03	2.428731E−03	8.746462E−07	+
	CLPSO	2.428064E−03	2.454903E−03	2.543269E−03	2.580951E−05	+
	BLPSO	2.425236E−03	2.437873E−03	2.488348E−03	1.372409E−05	+
	DE/BBO	2.428255E−03	2.461623E−03	2.525560E−03	2.925123E−05	+
	CMM-DE/BBO	**2.425075E−03**	2.425175E−03	2.426796E−03	3.554783E−07	≈

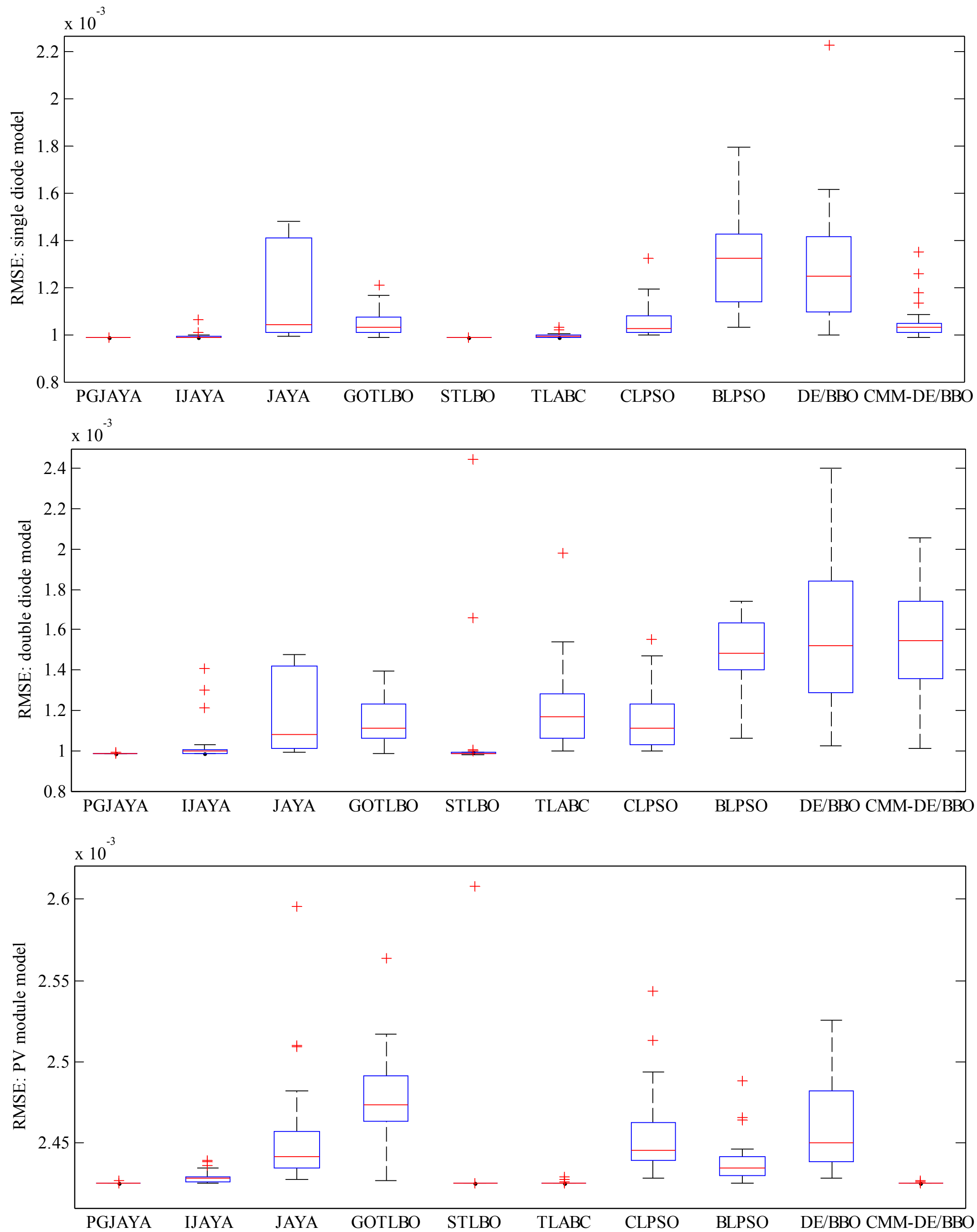

Fig. 3. Boxplot of best RMSE in 30 runs for RTC France PV cell and Photo Watt-PWP 201 PV module.

JAYA (IJAYA) [28], basic JAYA [32], generalized oppositional teaching-learning-based optimization (GOTLBO) [21], simplified TLBO (STLBO) [10], teaching-learning-based artificial bee colony (TLABC) [3], comprehensive learning particle swarm optimization (CLPSO) [50], biogeography-based learning particle swarm optimization (BLPSO) [51], differential evolution with biogeography-based optimization (DE/BBO) [52], and DE/BBO with covariance matrix based migration (CMM-DE/BBO) [53]. These nine algorithms are chosen for comparisons due to their good performance on parameters identification of PV cell and module models. The parameter configurations for all involved algorithms are given in Table 2. Please note that they are set according to the recommendations in the corresponding literatures. To make fair comparison among different algorithms, the same maximum number of function evaluations (FES_{max}) 50,000 is set to each algorithm in each run on each problem. Furthermore, to make the statistical comparisons, each algorithm is independently conducted 30 times on every problem.

In the first place, the performances in terms of accuracy, robustness,

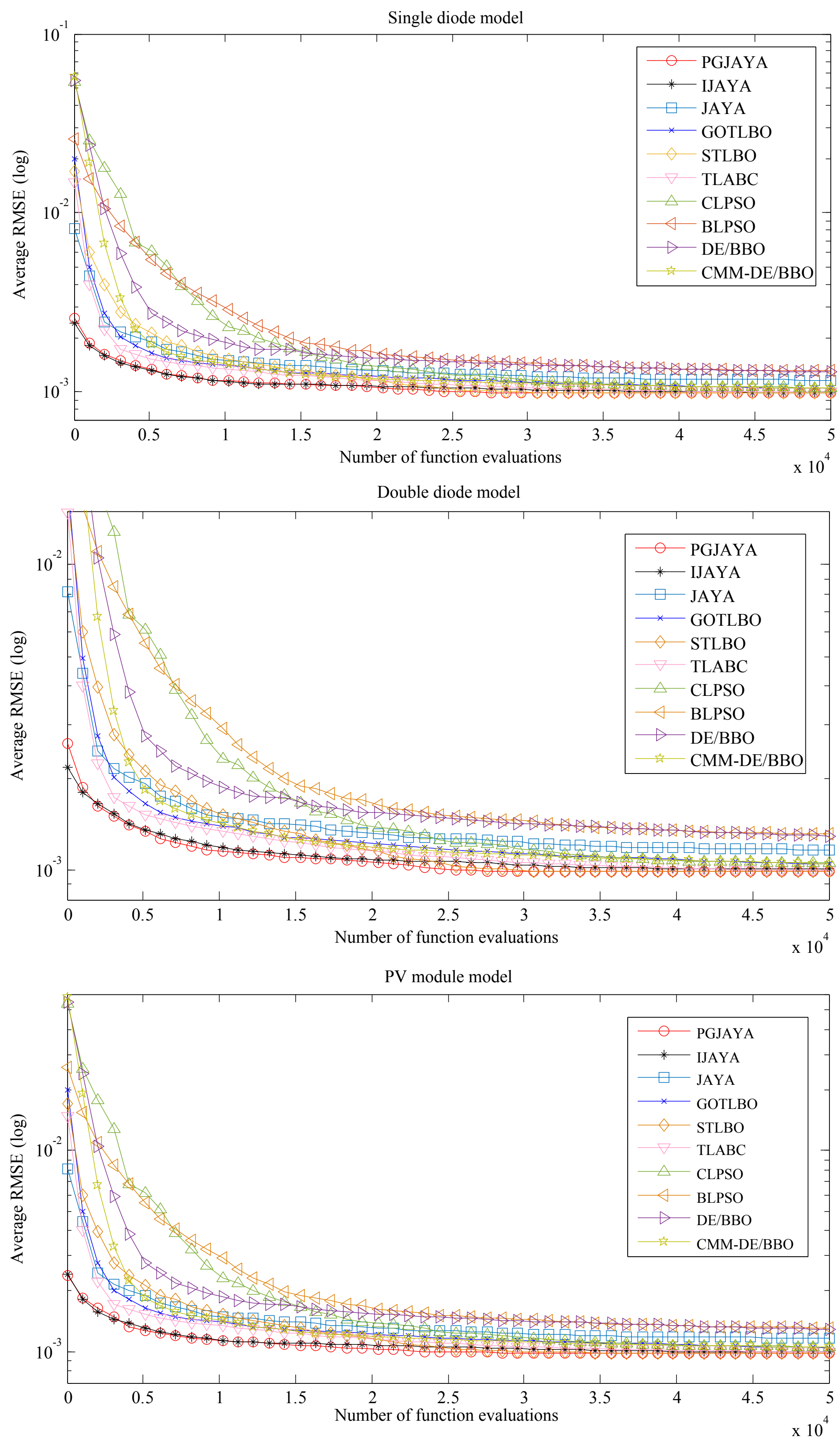

Fig. 4. Convergence curves of different algorithms for RTC France PV cell and Photo Watt-PWP 201 PV module.

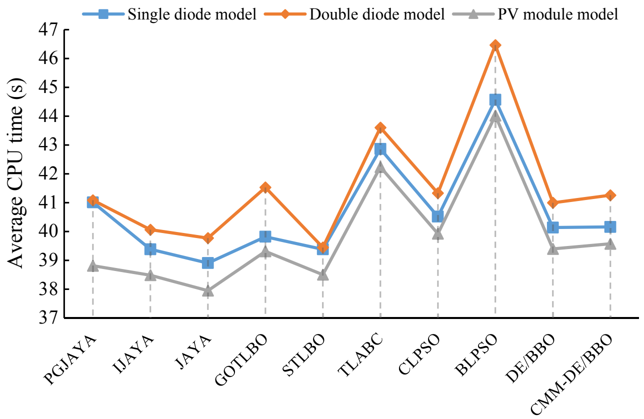

Fig. 5. The average CPU time of different algorithms for RTC France PV cell and Photo Watt-PWP 201 PV module.

Table 4
Detailed results for single diode model of RTC France.

Algorithm	$I_{ph}(A)$	$I_{sd}(\mu A)$	$R_S(\Omega)$	$R_{sh}(\Omega)$	n	RMSE
PGJAYA	0.7608	0.3230	0.0364	53.7185	1.4812	9.8602E−04
IJAYA	0.7608	0.3228	0.0364	53.7595	1.4811	9.8603E−04
JAYA	0.7608	0.3281	0.0364	54.9298	1.4828	9.8946E−04
GOTLBO	0.7608	0.3297	0.0363	53.3664	1.4833	9.8856E−04
STLBO	0.7608	0.3230	0.0364	53.7184	1.4812	9.8602E−04
TLABC	0.7608	0.3231	0.0364	53.7235	1.4812	9.8602E−04
CLPSO	0.7608	0.34302	0.0361	54.1965	1.4873	9.9633E−04
BLPSO	0.7607	0.36620	0.0359	60.2845	1.4939	1.0272E−03
DE/BBO	0.7605	0.32477	0.0364	55.2627	1.4817	9.9922E−04
CMM-DE/BBO	0.7608	0.32384	0.0364	53.8753	1.4814	9.8605E−04

and convergence rate of each algorithm are evaluated and compared by means of the statistical results and convergence curves. Afterwards, detailed comparisons are carried out based on the best RMSE values obtained by different methods in 30 runs. Note that the overall best RMSE values among all involved algorithms are marked in **boldface** in the following results.

5.1. Statistical results and convergence curves

In this subsection, the results obtained by different algorithms are compared through the statistical results and convergence curves. Table 3 lists the statistical results of all considered algorithms in 30 runs. The accuracy is reflected by minimum RMSE value, the average accuracy is indicated by mean RMSE value, the reliability is reflected by the standard deviation (SD) of RMSE. Besides, the Wilcoxon signed-rank test [54] with a significance level of 0.05 is employed to compare the significance between PGJAYA and its each competitor. In Table 3, symbols " + " and " ≈ " show the performance of PGJAYA is significantly better than and almost similar to that of the corresponding competitor, respectively.

From Table 3, it can be seen that PGJAYA has the best average accuracy and reliability on all three models due to it surpasses other nine algorithms regarding the mean RMSE and SD values. To be specific, for single diode model, although the minimum RMSE value is also found by STLBO and TLABC, their performances are worse than that of PGJAYA when considering the mean RMSE and SD. For double diode model, the best RMSE value is obtained by STLBO, however, its performance is unsteady since its mean RMSE and SD values are outperformed by PGJAYA. In fact, the best RMSE value found by PGJAYA is also competitive as it is the second best among all compared algorithms. For PV module model, PGJAYA, together with STLBO, TLABC, CMM-DE/BBO, get the best RMSE value. In terms of mean RMSE and SD values, the performance of CMM-DE/BBO is the second best among compared algorithms. When considering the statistical test results, as shown in the last column of Table 3, the superior performance of PGJAYA is also apparent. Both for single diode model and double diode model, PGJAYA achieves the significantly better results than its all competitors. For PV module model, the result of PGJAYA is almost similar to that of CMM-DE/BBO, and significantly surpasses the rest of eight algorithms. When compared with IJAYA, the superiority of PGJAYA is validated as it outperforms IJAYA in terms of all criterions on all three models. In particular, the performance of PGJAYA is also significant in view of statistical test results.

Moreover, in order to visually present the distribution of results obtained by different algorithms in 30 runs, the boxplot for each model is given in Fig. 3. Also, based on the comparisons on the solution distribution, it can be observed that the proposed PGJAYA exhibits the superior performance compared with other compared algorithms regarding accuracy and robustness.

The convergence curves of different algorithms for each model are presented in Fig. 4 to indicate the average RMSE performance in 30 independent runs. Compared with other algorithms, PGJAYA has the competitive or faster convergence rate, and this demonstrates that the searching process of PGJAYA is high-efficient.

In order to further demonstrate the computational efficiency of PGJAYA, the average computational time of all compared algorithms

Table 5
Detailed results for double diode model of RTC France.

Algorithm	$I_{ph}(A)$	$I_{sd1}(\mu A)$	$R_S(\Omega)$	$R_{sh}(\Omega)$	n_1	$I_{sd2}(\mu A)$	n_2	RMSE
PGJAYA	0.7608	0.21031	0.0368	55.8135	1.4450	0.88534	2.0000	9.8263E−04
IJAYA	0.7601	0.0050445	0.0376	77.8519	1.2186	0.75094	1.6247	9.8293E−04
JAYA	0.7607	0.0060763	0.0364	52.6575	1.8436	0.31507	1.4788	9.8934E−04
GOTLBO	0.7608	0.13894	0.0365	53.4058	1.7254	0.26209	1.4658	9.8742E−04
STLBO	0.7608	0.23364	0.0367	55.3382	1.4538	0.68494	2.0000	9.8252E−04
TLABC	0.7608	0.33673	0.0361	55.0676	1.4861	0.07173	1.9316	1.0012E−03
CLPSO	0.7607	0.25843	0.0367	57.9422	1.4625	0.38615	1.9435	9.9894E−04
BLPSO	0.7608	0.27189	0.0366	61.1345	1.4674	0.43505	1.9662	1.0628E−03
DE/BBO	0.7606	0.0012237	0.0358	58.4018	1.8791	0.37220	1.4956	1.0255E−03
CMM-DE/BBO	0.7607	0.35366	0.0360	57.9882	1.4907	0.025623	1.8835	1.0088E−03

Table 6
Detailed results for PV module model of Photo Watt-PWP 201.

Algorithm	$I_{ph}(A)$	$I_{sd}(\mu A)$	$R_S(\Omega)$	$R_{sh}(\Omega)$	n	RMSE
PGJAYA	1.0305	3.4818	1.2013	981.8545	48.6424	2.425075E−03
IJAYA	1.0305	3.4703	1.2016	977.3752	48.6298	2.425129E−03
JAYA	1.0302	3.4931	1.2014	1022.5	48.6531	2.427785E−03
GOTLBO	1.0307	3.5124	1.1995	969.9313	48.6766	2.426583E−03
STLBO	1.0305	3.4824	1.2013	982.0387	48.6430	2.425075E−03
TLABC	1.0305	3.4826	1.2013	982.1815	48.6432	2.425075E−03
CLPSO	1.0304	3.6131	1.1978	1017.0	48.7847	2.428064E−03
BLPSO	1.0305	3.5176	1.2002	992.7901	48.6815	2.425236E−03
DE/BBO	1.0303	3.6172	1.1969	1015.1	48.7894	2.428255E−03
CMM-DE/BBO	1.0305	3.4823	1.2013	981.9823	48.6428	2.425075E−03

Table 7
Comparison of PGJAYA with varying *NP* for RTC France PV cell and Photo Watt-PWP 201 PV module.

Model	Population size	RMSE			
		Min	Mean	Max	SD
Single diode model of RTC France	$NP = 10$	**9.860219E−04**	1.083912E−03	2.448049E−03	3.708204E−04
	$NP = 20$	**9.860219E−04**	**9.860224E−04**	**9.860293E−04**	**1.448469E−09**
	$NP = 30$	**9.860219E−04**	9.860236E−04	9.860480E−04	4.816731E−09
	$NP = 40$	**9.860219E−04**	9.861367E−04	9.889808E−04	5.383277E−07
Double diode model of RTC France	$NP = 10$	9.827309E−04	9.865883E−04	9.975999E−04	3.771774E−06
	$NP = 20$	**9.826271E−04**	**9.858217E−04**	**9.949852E−04**	**2.537520E−06**
	$NP = 30$	9.836123E−04	9.869291E−04	1.002713E−03	3.386724E−06
	$NP = 40$	9.827807E−04	9.883926E−04	1.009339E−03	5.743795E−06
PV module model of Photo Watt-PWP 201	$NP = 10$	**2.425075E−03**	1.148639E−02	2.742508E−01	4.962827E−02
	$NP = 20$	**2.425075E−03**	**2.425144E−03**	2.426764E−03	3.071420E−07
	$NP = 30$	**2.425075E−03**	2.425167E−03	**2.425747E−03**	**2.000078E−07**
	$NP = 40$	**2.425075E−03**	2.425195E−03	2.426102E−03	2.644553E−07

on three models are compared. The mean CPU time for each algorithm on each model in the 30 runs is recorded. Please note that all algorithms are implemented in MATLAB R2014a, and experiments are performed in a server with Windows 7 system, Intel Xeon 2.60 GHz CPU, and 128 GB RAM. From the results shown in Fig. 5, it can be seen that different computational time are needed to solve different problems for each algorithm. To be specific, on each model, a longer computational time is required by BLPSO when comparing with the other algorithms, while the lowest computational overhead is consumed by JAYA among all compared algorithms. Also, PGJAYA shows the competitive or superior performance as it consumes a less computational time than most of the other algorithms on each model. When compared with IJAYA, although a litter more time is consumed by PGJAYA, this is worthy as significant better results are obtained by PGJAYA as shown in Table 3. The comparison implies that the proposed PGJAYA can get the superior results with fairly satisfactory computational efficiency.

As a summary, the above comparisons indicate that PGJAYA has better searching accuracy, robustness, and faster convergence rate in identifying the model parameters of PV cell and module. Moreover, when comparing with other state-of-the-art algorithms, the performance of PGJAYA is competitive.

5.2. Detailed results comparison

In order to further analysis the results, the best RMSE value and the corresponding parameters extracted by different algorithms are compared in detail. Please note that some Tables and Figures are presented in Appendix A to make the paper easy to read.

5.2.1. Results on single diode model of RTC France

As shown in Table 4, the extracted five parameters and the corresponding RMSE values for single diode model are given to compare. We can see that the best RMSE value (9.8602E−04) is obtained by PGJAYA, STLBO, and TLABC, while the worst RMSE value (1.0272E−03) is found by BLPSO. Considering that no prior information for the accurate parameter values is available, so the RMSE value is selected as an indicator to represent the accuracy of estimating parameters. Although the RMSE values obtained by other algorithms except BLPSO are close to that found by PGJAYA, any reduction on RMSE is significant since it gets improvement in the knowledge on the actual parameters values. In addition, to verify the accuracy of optimal parameter values estimated by PGJAYA, the individual absolute errors (IAE) of current and power between the experimental data and calculated data are shown in Table A1 of appendix and illustrated in Fig. A1, respectively. It can be seen that all IAE values on current are not more than 2.51E−03 and those on power are less than1.46E−03. In addition, the *I-V* and *P-V* characteristics in Fig. A1 indicate that the calculated data obtained by PGJAYA are in well agreement with the experimental data over the whole voltage range. These provide sufficient evidence that the parameters extracted by PGJAYA are very accurate.

5.2.2. Results on double diode model of RTC France

As presented in Table 5, the estimated seven parameters and the related RMSE values for double diode model obtained by different algorithms are summarized. We can observe that the performance of STLBO is the best one as it gets the smallest RMSE value (9.8252E−04), and the performance of PGJAYA is also competitive due to it provides

Table 8
Estimated optimal parameters by PGJAYA for three types of PV modules at different irradiance and temperature of 25 °C.

Parameters	Thin-film ST40	Mono-crystalline SM55	Multi-crystalline KC200GT
G = 1000 W/m^2			
$I_{ph}(A)$	2.67575018	3.45009071	8.21666157
$I_{sd}(\mu A)$	1.53296620	0.17147816	0.00228368
$R_S(\Omega)$	1.11305759	0.32908497	0.34351050
$R_{sh}(\Omega)$	358.244278	484.362104	773.811733
n	1.50055956	1.39590894	1.07729991
RMSE	0.00073423	0.00114625	0.00154545
G = 800 W/m^2			
$I_{ph}(A)$	2.13795511	2.76038319	6.57077894
$I_{sd}(\mu A)$	1.16740687	0.14387466	0.00098289
$R_S(\Omega)$	1.12459343	0.33762003	0.35685812
$R_{sh}(\Omega)$	333.622982	459.822669	764.396583
n	1.47395734	1.38110188	1.03672056
RMSE	0.00077437	0.00066858	0.00164845
G = 600 W/m^2			
$I_{ph}(A)$	1.60480832	2.07088885	4.93392066
$I_{sd}(\mu A)$	1.44214839	0.15582472	0.00411733
$R_S(\Omega)$	1.11259106	0.33037911	0.33576355
$R_{sh}(\Omega)$	347.715235	450.308497	762.626052
n	1.49584106	1.38770174	1.10739238
RMSE	0.00067403	0.00082396	0.00134323
G = 400 W/m^2			
$I_{ph}(A)$	1.06754286	1.38284163	3.28769104
$I_{sd}(\mu A)$	1.84935147	0.10050615	0.00160717
$R_S(\Omega)$	1.08052378	0.39655034	0.35044054
$R_{sh}(\Omega)$	362.537971	427.112916	762.735516
n	1.52449182	1.35205736	1.05872504
RMSE	0.00063072	0.00070761	0.00144082
G = 200 W/m^2			
$I_{ph}(A)$	0.53313758	0.69150897	1.6459051
$I_{sd}(\mu A)$	1.42956635	0.14650976	0.00053721
$R_S(\Omega)$	1.18576145	0.28641982	0.37895129
$R_{sh}(\Omega)$	344.981298	448.231466	697.737767
n	1.49751278	1.38071890	1.00463136
RMSE	0.00047772	0.00032068	0.00141852

the second smallest result (9.8263E − 04). As a contrast, inferior RMSE values are found by remaining algorithms, especially the RMSE value obtained by BLPSO is the worst one. Furthermore, the experimental and calculated data are compared in Table A2 and Fig. A2 to validate the accuracy of optimal parameter values extracted by PGJAYA. From Table A2, we can see that all IAE values on current are smaller than 2.55E − 03 and those on power are less than 1.49E − 03, which demonstrate that the high-accurately parameters are estimated by PGJAYA. Besides, it is clear from Fig. A2 that the calculated data are in excellent accordance with the experimental data.

In addition, by comparing the results of single and double diode models obtained by PGJAYA (Tables A1 and A2), we can observe that the RMSE value and the sum of IAE on calculated current of double diode model are smaller than those of single diode model. This further verifies that high accurate parameter values are estimated by PGJAYA. Nevertheless, about the calculated power data, the sum of IAE of double diode model is larger than that of single diode model, which because that the objective function in this study is to minimize the errors between the calculated and experimental current data instead of the power data. Thereby, objective function for parameters estimation of PV models can be selected and designed according to the specific application and requirement.

5.2.3. Results on PV module model of Photo Watt-PWP 201

As shown in Table 6, the estimated five parameters and the related RMSE values for PV module model found by different algorithms are listed. We can see that the best RMSE value (2.425075E − 03) is obtained by PGJAYA, STLBO, TLABC, and CMM-DE/BBO, while the second best RMSE value is found by IJAYA. Similarly, the calculated data found by PGJAYA and experimental data are compared in Table A3 and Fig. A3. It is obvious from *I-V* and *P-V* characteristics that the calculated data match the experimental data very well. The absolute error on current and power, and their sum are very tiny when comparing with the experimental current data and power data. These comparisons prove that high accuracy parameters are estimated again by PGJAYA.

5.3. Discussions of different population sizes

In this subsection, more experiments are carried out to discuss the influence of population size *NP* on the performance of the proposed PGJAYA algorithm. To this end, PGJAYA with *NP* = 10, 20, 30, and 40 are tested and compared. It is worth noting that the maximum number of function evaluations is kept the same as that in preceding experiments of this study. The statistical results of PGJAYA in 30 independent runs with varying *NP* are presented in Table 7. The comparison results show that smaller value for *NP* (i.e., 10) will lead to the inferior results in terms of the mean RMSE values and the standard deviation. In contrast, when the population size *NP* is relatively bigger (i.e., 30 and 40), the performance of PGJAYA will deteriorate for three models. This is because that the problems considered in this study belong to low dimension problem, and if the population size is too large, the number of iterations will be lower when the maximum number of function

Table 9
Estimated optimal parameters by PGJAYA for three modules at different temperature and irradiance of 1000 W/m^2.

PV modules	Temperature	$I_{ph}(A)$	$I_{sd}(\mu A)$	$R_S(\Omega)$	$R_{sh}(\Omega)$	n	RMSE
Thin-film ST40	25 °C	2.67575018	1.53296620	1.11305759	358.244278	1.50055956	0.00073423
	40 °C	2.68085240	5.68929264	1.12899786	365.056451	1.47693328	0.00132157
	55 °C	2.69184344	18.84550870	1.14892118	296.681681	1.45083115	0.00182369
	70 °C	2.69232435	87.54708884	1.12586455	367.871810	1.48060051	0.00077771
Mono-crystalline SM55	25 °C	3.45009071	0.17147816	0.32908497	484.362104	1.39590894	0.00114625
	40 °C	3.46937727	1.06771183	0.31754537	521.245250	1.41143624	0.00346534
	60 °C	3.49460590	6.91033742	0.31870086	484.96740196	1.40515457	0.00378038
Multi-crystalline KC200GT	25 °C	8.21666157	0.00228368	0.34351050	773.811733	1.07729991	0.00154545
	50 °C	8.29520784	0.12649049	0.33557361	861.929728	1.11755287	0.00274698
	75 °C	8.37750630	1.64166410	0.34237090	802.4583974	1.10194835	0.00447384

evaluations has been determined, this is unfavorable for the low dimension problems. When *NP* is 20, the overall performance of PGJAYA is the best for three models. Hence, the aforementioned comparisons indicate that $NP = 20$ is the most appropriate parameter setting for PGJAYA on the three models.

5.4. Results of experimental data from the manufacturer's data sheet

In this subsection, the practicability and reliability of the proposed PGJAYA is further evaluated using experimental data obtained from the manufacturer's data sheet of three PV modules with different types: Thin-film (ST40), Mono-crystalline (SM55), and Multi-crystalline (KC200GT) [24]. The used experimental data are directly extracted from the current-voltage curves given in the manufacturer's data sheets at five different irradiation levels (1000 W/m^2, 800 W/m^2, 600 W/m^2, 400 W/m^2, and 200 W/m^2), and different temperature levels. The search range of the unknown parameters are given as $I_{ph} \in [0,\ 2I_{SC}](\mathrm{A})$, $I_{sd} \in [0,\ 100](\mu\mathrm{A})$, $R_S \in [0,\ 2](\Omega)$, $R_{sh} \in [0,\ 5000](\Omega)$ and $n \in [1,\ 4]$. As shown in Eq. (19), the I_{SC} at non-standard test condition is determined by the data sheet parameters at standard test condition (*STC*): short circuit current I_{SC_STC}, temperature coefficient for short circuit current α [26].

$$I_{SC}(G,\ T) = I_{SC\_STC}\frac{G}{G_{STC}} + \alpha(T - T_{STC}) \tag{19}$$

where G and T denote the irradiance and temperature levels, respectively.

The optimal identified parameters of the single diode model for three types of PV modules, at different levels of irradiation and a constant value of temperature, are listed in Table 8. Furthermore, in order to illustrate the accuracy of the estimated optimal parameters of the PV modules, the estimated current is calculated and the *I-V* characteristics of the three different modules are plotted at different irradiation levels as given in Fig. A4. Meanwhile, the optimal identified parameters for three types of PV modules, at different levels of temperature and a constant value of irradiation, are shown in Table 9. The comparisons between the calculated data and the experimental data are presented in Fig. A5. From the results, it can be observed that, for all the three types of PV modules, the *I-V* characteristics obtained from the identified optimal parameters are very close to the experimental data, under different irradiance and temperature levels. In particular, from Table 8, the proposed method achieves accurate estimation of the PV modules parameters at low irradiance as a low RMSE is obtained. In fact, in these circumstances, the module is subjected to certain mismatch conditions such as partial shading.

In addition, the optimal extracted results agree well with those achieved by other parameter estimation methods [24,26,55,56]. From Tables 8 and 9, it can be observed that the estimation parameters I_{ph} and I_{sd} are changed as the conditions varying, while parameters R_S, R_{sh}, and n are kept to be nearly constant under different conditions. To be specific, from the physical perspective, parameter I_{ph} is the photocurrent and its value will be increased as the irradiance level increasing. Obviously, this phenomenon is demonstrated by the results shown in Table 8. Parameter I_{sd} is the reverse saturation current of diode and its value is positively related to the temperature. The increase in I_{sd} is because of the enhancement of photon absorption with increased temperature [57], and this is also validated by the results presented in Table 9. Moreover, it can be seen that the value of the series resistance R_S for Thin-film is around 1 and less than 0.4 for both Mono-crystalline and Multi-crystalline. All this indicates that the values of model parameters are observed to be nearly constant for all environmental conditions matching exactly with the theoretical prediction of smaller series resistance and higher parallel resistance [55]. For the diode ideality factor n, its value is kept to be nearly constant for one specific model under different conditions, but its value is different for different kinds of PV models. As an example, for multi-crystalline KC200GT, its n value is closing to 1 as this kind of PV model is diffusion-guided device. In summary, the above discussions indicate that the extracted parameters under different conditions by the proposed algorithm are accurate and reasonable from the physics points of view.

6. Conclusions

In this study, a performance-guided JAYA (PGJAYA) algorithm is proposed to estimate the model parameters of PV cell and module. In PGJAYA algorithm, the individual performance in the population is quantified by probability first. Then, based on probability, each individual self-adaptively selects the appropriate evolution strategy designed for promoting exploration or exploitation ability to perform the searching process. Also, the quantified performance is used to choose the exemplar to construct the promising searching direction. Furthermore, to improve the quality of whole population, a self-adaptive chaotic perturbation mechanism is introduced to explore more better solution around the current best solution for replacing the worst one. Extensive experiments are carried out to evaluate the performance of PGJAYA in identifying parameters of different PV models including single diode, double diode, and PV module. Experimental results and comparisons verify the competitive and superior performance of PGJAYA regarding accuracy and robustness compared with other well-established algorithms. In addition, the influence of population size to the performance of PGJAYA is investigated. Finally, experiments on three PV modules of different types at different irradiance levels and different temperature values further validate that the proposed PGJAYA is effective and practical. Therefore, the proposed PGJAYA is a hopeful candidate method for extracting model parameters of PV cell and module. Also, PGJAYA can be viewed as an efficient technique to deal with other optimization problems in energy system.

Future work will include demonstrating the robustness of the proposed algorithm when fitting the data set with some degree of noise, and extending the method application to other fields involving rough data collection. Furthermore, attempts will be made to explore the applied values of heuristic methods for other energy optimization problems [58–60].

Acknowledgments

This work was supported by the National Natural Science Foundation of China (61806179, 61876169, 61473266, and 61673404), China Postdoctoral Science Foundation (2017M622373), Key R&D and Promotion Projects in Henan Province (192102210405), Fundamental Research Funds for the Central Universities (222201817006), Program for Science & Technology Innovation Talents in Universities of Henan Province (16HASTIT041 and 16HASTIT033), China Textile Industry Association Science and Technology Guidance Project (2017054), and Young Backbone Teachers of Henan Province (2016GGJS-094).

Appendix A

See Figs. A1–A5 and Tables A1–A3.

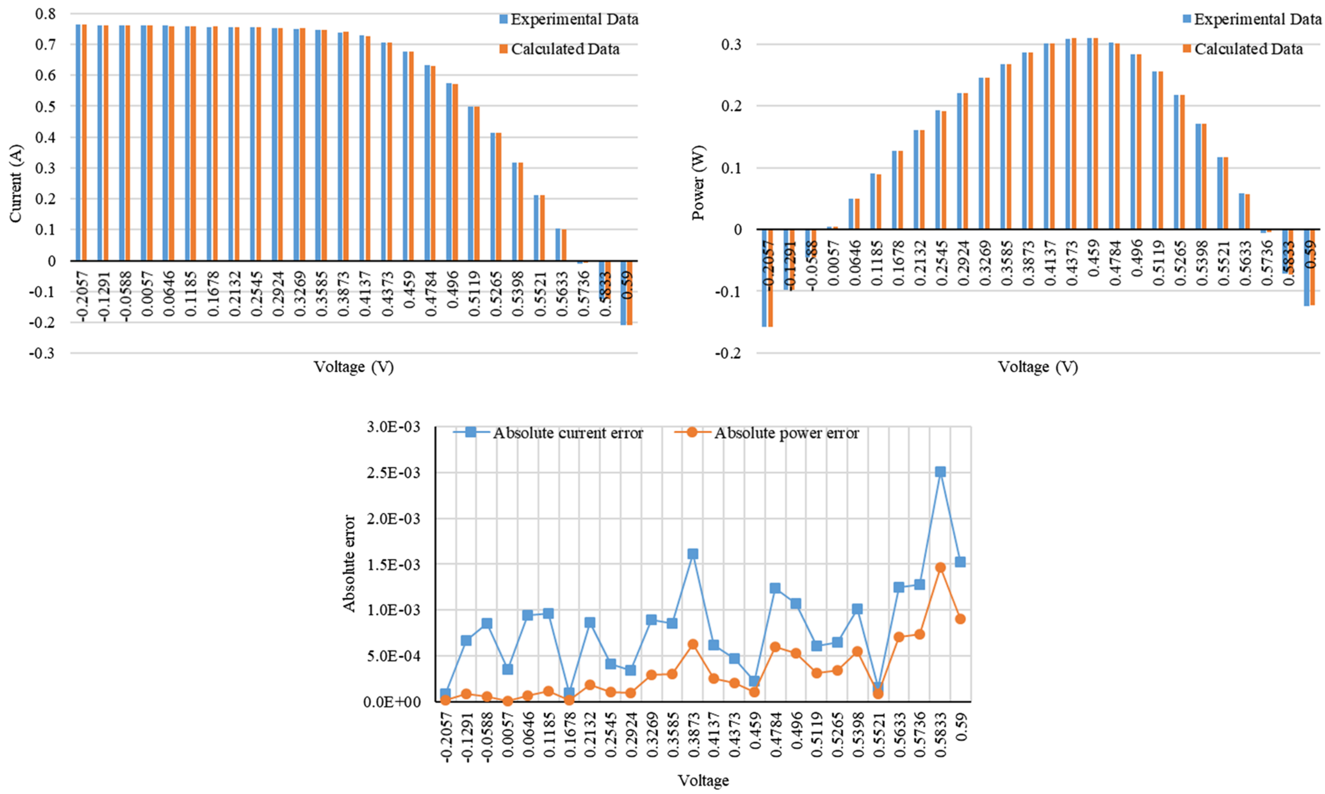

Fig. A1. Comparisons between experimental and calculated data of PGJAYA for single diode model of RTC France.

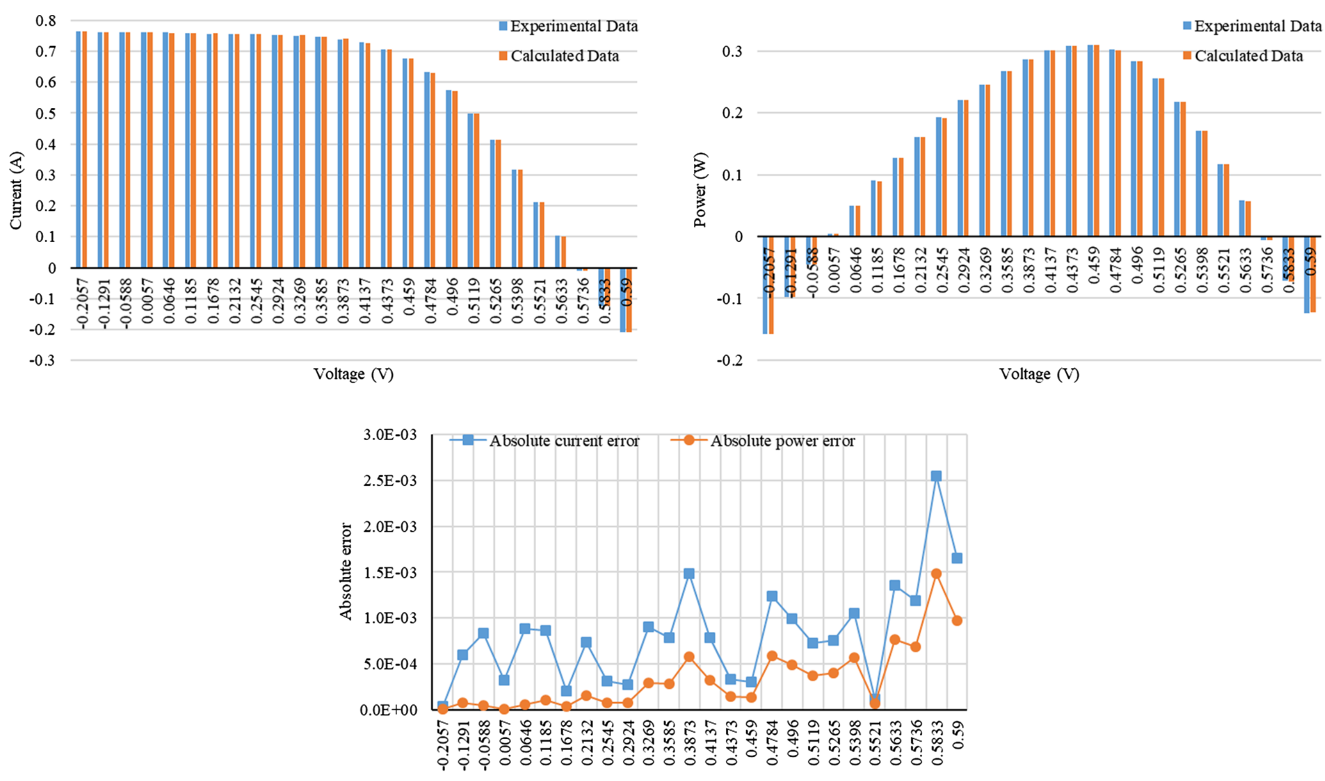

Fig. A2. Comparisons between experimental and calculated data of PGJAYA for double diode model of RTC France.

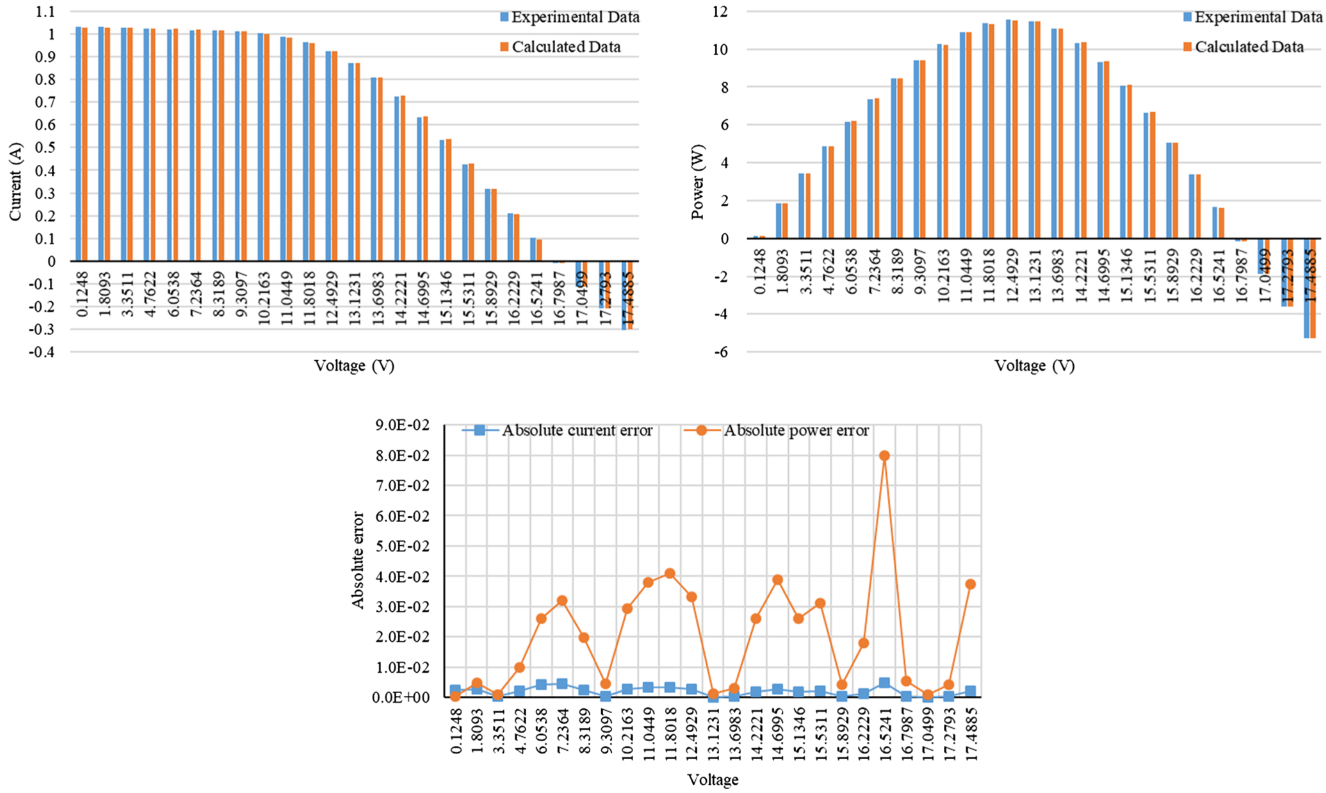

Fig. A3. Comparisons between experimental and calculated data of PGJAYA for PV module model of Photo Watt-PWP 201.

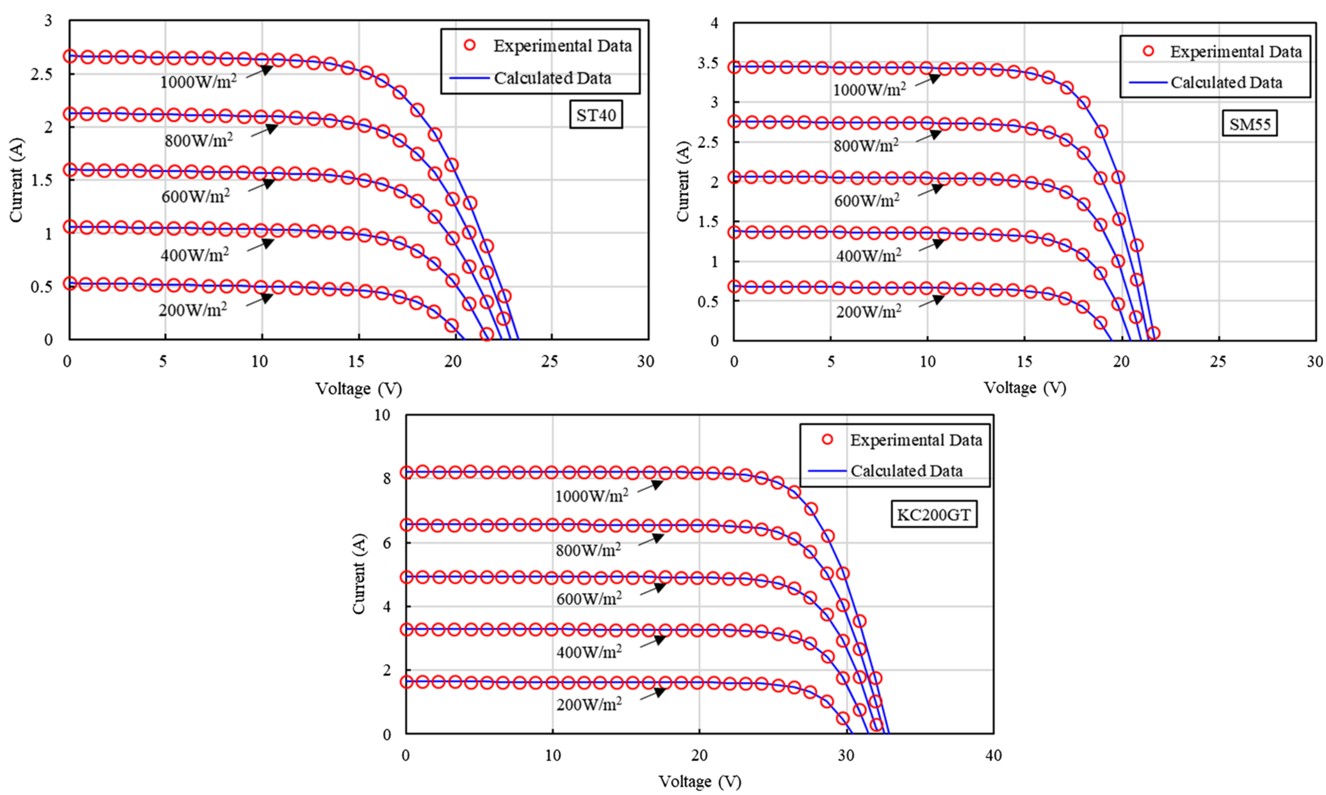

Fig. A4. Comparisons between experimental and calculated data for three types modules at different irradiance.

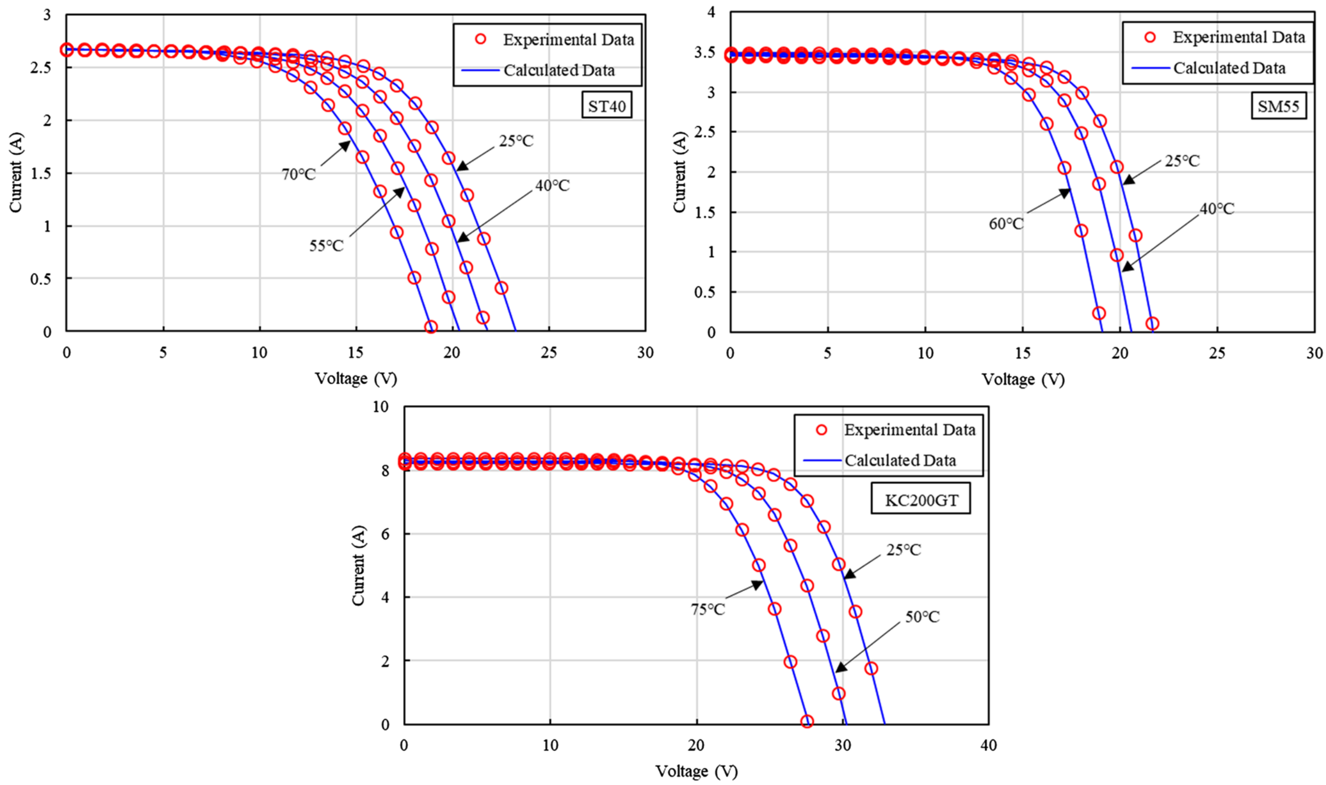

Fig. A5. Comparisons between experimental and calculated data for three types modules at different temperature.

Table A1
IAE of PGJAYA for single diode model of RTC France.

Item	Experimental data		Calculated current data		Calculated power data	
	V (V)	I (A)	I_{sim} (A)	IAE_I (A)	P_{sim} (W)	IAE_P (W)
1	−0.2057	0.7640	0.76408771	0.00008771	−0.15717284	0.00001804
2	−0.1291	0.7620	0.76266309	0.00066309	−0.09845980	0.00008560
3	−0.0588	0.7605	0.76135531	0.00085531	−0.04476769	0.00005029
4	0.0057	0.7605	0.76015399	0.00034601	0.00433288	0.00000197
5	0.0646	0.7600	0.75905521	0.00094479	0.04903497	0.00006103
6	0.1185	0.7590	0.75804234	0.00095766	0.08982802	0.00011348
7	0.1678	0.7570	0.75709165	0.00009165	0.12703998	0.00001538
8	0.2132	0.7570	0.75614136	0.00085864	0.16120934	0.00018306
9	0.2545	0.7555	0.75508687	0.00041313	0.19216961	0.00010514
10	0.2924	0.7540	0.75366387	0.00033613	0.22037132	0.00009828
11	0.3269	0.7505	0.75139096	0.00089096	0.24562971	0.00029126
12	0.3585	0.7465	0.74735385	0.00085385	0.26792635	0.00030610
13	0.3873	0.7385	0.74011722	0.00161722	0.28664740	0.00062635
14	0.4137	0.7280	0.72738222	0.00061778	0.30091803	0.00025557
15	0.4373	0.7065	0.70697265	0.00047265	0.30915914	0.00020669
16	0.4590	0.6755	0.67528016	0.00021984	0.30995359	0.00010091
17	0.4784	0.6320	0.63075828	0.00124172	0.30175476	0.00059404
18	0.4960	0.5730	0.57192836	0.00107164	0.28367647	0.00053153
19	0.5119	0.4990	0.49960702	0.00060702	0.25574883	0.00031073
20	0.5265	0.4130	0.41364879	0.00064879	0.21778609	0.00034159
21	0.5398	0.3165	0.31751011	0.00101011	0.17139196	0.00054526
22	0.5521	0.2120	0.21215493	0.00015493	0.11713074	0.00008554
23	0.5633	0.1035	0.10225131	0.00124869	0.05759816	0.00070339
24	0.5736	−0.0100	−0.00871755	0.00128245	−0.00500038	0.00073562
25	0.5833	−0.1230	−0.12550741	0.00250741	−0.07320847	0.00146257
26	0.5900	−0.2100	−0.20847232	0.00152768	−0.12299867	0.00090133
Sum of IAE				0.02152687		0.00873078

Table A2
IAE of PGJAYA for double diode model of RTC France.

Item	Experimental data		Calculated current data		Calculated power data	
	V (V)	I (A)	I_{sim} (A)	IAE_I (A)	P_{sim} (W)	IAE_P (W)
1	−0.2057	0.7640	0.76396536	0.00003464	−0.15714767	0.00000713
2	−0.1291	0.7620	0.76259413	0.00059413	−0.09845090	0.00007670
3	−0.0588	0.7605	0.76133513	0.00083513	−0.04476651	0.00004911
4	0.0057	0.7605	0.76017790	0.00032210	0.00433301	0.00000184
5	0.0646	0.7600	0.75911761	0.00088239	0.04903900	0.00005700
6	0.1185	0.7590	0.75813605	0.00086395	0.08983912	0.00010238
7	0.1678	0.7570	0.75720632	0.00020632	0.12705922	0.00003462
8	0.2132	0.7570	0.75626202	0.00073798	0.16123506	0.00015734
9	0.2545	0.7555	0.75519318	0.00030682	0.19219666	0.00007809
10	0.2924	0.7540	0.75373188	0.00026812	0.22039120	0.00007840
11	0.3269	0.7505	0.75139886	0.00089886	0.24563229	0.00029384
12	0.3585	0.7465	0.74728955	0.00078955	0.26790330	0.00028305
13	0.3873	0.7385	0.73998866	0.00148866	0.28659761	0.00057656
14	0.4137	0.7280	0.72722015	0.00077985	0.30085098	0.00032262
15	0.4373	0.7065	0.70682714	0.00032714	0.30909551	0.00014306
16	0.4590	0.6755	0.67519893	0.00030107	0.30991631	0.00013819
17	0.4784	0.6320	0.63076419	0.00123581	0.30175759	0.00059121
18	0.4960	0.5730	0.57201096	0.00098904	0.28371744	0.00049056
19	0.5119	0.4990	0.49972822	0.00072822	0.25581088	0.00037278
20	0.5265	0.4130	0.41375155	0.00075155	0.21784019	0.00039569
21	0.5398	0.3165	0.31755272	0.00105272	0.17141496	0.00056826
22	0.5521	0.2120	0.21211444	0.00011444	0.11710838	0.00006318
23	0.5633	0.1035	0.10214275	0.00135725	0.05753701	0.00076454
24	0.5736	−0.0100	−0.00880873	0.00119127	−0.00505268	0.00068332
25	0.5833	−0.1230	−0.12555095	0.00255095	−0.07323387	0.00148797
26	0.5900	−0.2100	−0.20834861	0.00165139	−0.12292568	0.00097432
Sum of IAE				0.02125936		0.00879173

Table A3
IAE of PGJAYA for PV module model of Photo Watt-PWP 201.

Item	Experimental data		Calculated current data		Calculated power data	
	V (V)	I (A)	I_{sim} (A)	IAE_I (A)	P_{sim} (W)	IAE_P (W)
1	0.1248	1.0315	1.02911964	0.00238036	0.12843413	0.00029707
2	1.8093	1.0300	1.02738133	0.00261867	1.85884105	0.00473795
3	3.3511	1.0260	1.02574186	0.00025814	3.43736354	0.00086506
4	4.7622	1.0220	1.02410704	0.00210704	4.87700256	0.01003416
5	6.0538	1.0180	1.02229155	0.00429155	6.18874858	0.02598018
6	7.2364	1.0155	1.01993032	0.00443032	7.38062378	0.03205958
7	8.3189	1.0140	1.01636269	0.00236269	8.45501961	0.01965501
8	9.3097	1.0100	1.01049575	0.00049575	9.40741231	0.00461531
9	10.2163	1.0035	1.00062866	0.00287134	10.22272257	0.02933448
10	11.0449	0.9880	0.98454823	0.00345177	10.87423671	0.03812449
11	11.8018	0.9630	0.95952173	0.00347827	11.32408356	0.04104984
12	12.4929	0.9255	0.92283908	0.00266092	11.52893638	0.03324257
13	13.1231	0.8725	0.87260009	0.00010009	11.45121830	0.00131355
14	13.6983	0.8075	0.80727477	0.00022523	11.05829198	0.00308527
15	14.2221	0.7265	0.72833695	0.00183695	10.35848100	0.02612535
16	14.6995	0.6345	0.63713835	0.00263835	9.36561516	0.03878241
17	15.1346	0.5345	0.53621321	0.00171321	8.11537252	0.02592882
18	15.5311	0.4275	0.42951127	0.00201127	6.67078249	0.03123724
19	15.8929	0.3185	0.31877424	0.00027424	5.06624708	0.00435843
20	16.2229	0.2085	0.20738914	0.00111086	3.36445321	0.01802144
21	16.5241	0.1010	0.09616674	0.00483326	1.58906885	0.07986525
22	16.7987	−0.0080	−0.00832571	0.00032571	−0.13986104	0.00547144
23	17.0499	−0.1110	−0.11093663	0.00006337	−1.89145840	0.00108050
24	17.2793	−0.2090	−0.20924715	0.00024715	−3.61564422	0.00427052
25	17.4885	−0.3030	−0.30086309	0.00213691	−5.26164421	0.03737129
Sum of IAE				0.04892343		0.51690722

References

[1] Das UK, Tey KS, Idris MYI, Mekhilef S, Seyedmahmoudian M, Horan B, et al. Forecasting of photovoltaic power generation and model optimization: a review. Renew Sustain Energy Rev 2018;81:912–28.
[2] Li Z, Zang C, Zeng P, Yu H, Li S. Fully distributed hierarchical control of parallel grid-supporting inverters in islanded AC microgrids. IEEE Trans Ind Inf 2018;14:679–90.
[3] Chen X, Xu B, Mei C, Ding Y, Li K. Teaching–learning–based artificial bee colony for solar photovoltaic parameter estimation. Appl Energy 2018;212:1578–88.
[4] Zhou S, Wang J. Dual serial vortex-induced energy harvesting system for enhanced energy harvesting. Aip Adv 2018;8.
[5] Gao X, Cui Y, Hu J, Xu G, Wang Z, Qu J, et al. Parameter extraction of solar cell

models using improved shuffled complex evolution algorithm. Energy Convers Manage 2018;157:460–79.
[6] Campana PE, Wästhage L, Nookuea W, Tan Y, Yan J. Optimization and assessment of floating and floating-tracking PV systems integrated in on- and off-grid hybrid energy systems. Sol Energy 2019;177:782–95.
[7] Allam D, Yousri DA, Eteiba MB. Parameters extraction of the three diode model for the multi-crystalline solar cell/module using Moth-Flame Optimization Algorithm. Energy Convers Manage 2016;123:535–48.
[8] Jiang LL, Maskell DL, Patra JC. Parameter estimation of solar cells and modules using an improved adaptive differential evolution algorithm. Appl Energy 2013;112:185–93.
[9] Ortiz-Conde A, Sánchez FJG, Muci J. New method to extract the model parameters of solar cells from the explicit analytic solutions of their illuminated I-V characteristics. Sol Energy Mater Sol Cells 2006;90:352–61.
[10] Niu Q, Zhang H, Li K. An improved TLBO with elite strategy for parameters identification of PEM fuel cell and solar cell models. Int J Hydrogen Energy 2014;39:3837–54.
[11] Yu K, Chen X, Wang X, Wang Z. Parameters identification of photovoltaic models using self-adaptive teaching-learning-based optimization. Energy Convers Manage 2017;145:233–46.
[12] Niu Q, Zhang L, Li K. A biogeography-based optimization algorithm with mutation strategies for model parameter estimation of solar and fuel cells. Energy Convers Manage 2014;86:1173–85.
[13] Ma J, Bi Z, Ting TO, Hao S, Hao W. Comparative performance on photovoltaic model parameter identification via bio-inspired algorithms. Sol Energy 2016;132:606–16.
[14] Humada AM, Hojabri M, Mekhilef S, Hamada HM. Solar cell parameters extraction based on single and double-diode models: a review. Renew Sustain Energy Rev 2016;56:494–509.
[15] Jordehi AR. Enhanced leader particle swarm optimisation (ELPSO): an efficient algorithm for parameter estimation of photovoltaic (PV) cells and modules. Sol Energy 2018;159:78–87.
[16] Nunes HGG, Pombo JAN, Mariano SJPS, Calado MRA, Souza JAMFD. A new high performance method for determining the parameters of PV cells and modules based on guaranteed convergence particle swarm optimization. Appl Energy 2018;211:774–91.
[17] Zagrouba M, Sellami A, Bouaïcha M, Ksouri M. Identification of PV solar cells and modules parameters using the genetic algorithms: application to maximum power extraction. Sol Energy 2010;84:860–6.
[18] Gong W, Cai Z. Parameter extraction of solar cell models using repaired adaptive differential evolution. Sol Energy 2013;94:209–20.
[19] Jamadi M, Merrikh-Bayat F, Bigdeli M. Very accurate parameter estimation of single-and double-diode solar cell models using a modified artificial bee colony algorithm. Int J Energy Environ Eng 2016;7:13–25.
[20] Oliva D, Cuevas E, Pajares G. Parameter identification of solar cells using artificial bee colony optimization. Energy 2014;72:93–102.
[21] Chen X, Yu K, Du W, Zhao W, Liu G. Parameters identification of solar cell models using generalized oppositional teaching learning based optimization. Energy 2016;99:170–80.
[22] Askarzadeh A, Rezazadeh A. Parameter identification for solar cell models using harmony search-based algorithms. Sol Energy 2012;86:3241–9.
[23] Wu Z, Yu D, Kang X. Parameter identification of photovoltaic cell model based on improved ant lion optimizer. Energy Convers Manage 2017;151:107–15.
[24] Xu S, Wang Y. Parameter estimation of photovoltaic modules using a hybrid flower pollination algorithm. Energy Convers Manage 2017;144:53–68.
[25] Ram JP, Babu TS, Dragicevic T, Rajasekar N. A new hybrid bee pollinator flower pollination algorithm for solar PV parameter estimation. Energy Convers Manage 2017;135:463–76.
[26] Alam DF, Yousri DA, Eteiba MB. Flower Pollination Algorithm based solar PV parameter estimation. Energy Convers Manage 2015;101:410–22.
[27] Oliva D, El Aziz MA, Hassanien AE. Parameter estimation of photovoltaic cells using an improved chaotic whale optimization algorithm. Appl Energy 2017;200:141–54.
[28] Yu K, Liang J, Qu B, Chen X, Wang H. Parameters identification of photovoltaic models using an improved JAYA optimization algorithm. Energy Convers Manage 2017;150:742–53.
[29] Yuan X, Xiang Y, He Y. Parameter extraction of solar cell models using mutative-scale parallel chaos optimization algorithm. Sol Energy 2014;108:238–51.
[30] Askarzadeh A, Rezazadeh A. Artificial bee swarm optimization algorithm for parameters identification of solar cell models. Appl Energy 2013;102:943–9.
[31] Fathy A, Rezk H. Parameter estimation of photovoltaic system using imperialist competitive algorithm. Renewable Energy 2017;111:307–20.
[32] Rao RV. Jaya: a simple and new optimization algorithm for solving constrained and unconstrained optimization problems. Int J Ind Eng Comput 2016;7:19–34.
[33] Rao V, Keesari HS. Multi-team perturbation guiding Jaya algorithm for optimization of wind farm layout. Appl Soft Comput 2018.
[34] Gao K, Yang F, Zhou M, Pan Q, Suganthan PN. Flexible job-shop rescheduling for new job insertion by using discrete Jaya algorithm. IEEE Trans Cybernet 2018.
[35] Wang L, Zhang Z, Huang C, Tsui KL. A GPU-accelerated parallel Jaya algorithm for efficiently estimating Li-ion battery model parameters. Appl Soft Comput 2018;65:12–20.
[36] Huang C, Wang L, Yeung RS-C, Zhang Z, Chung HS-H, Bensoussan A. A prediction model-guided Jaya algorithm for the PV system maximum power point tracking. IEEE Trans Sustain Energy 2018;9:45–55.
[37] Rao R, More K. Design optimization and analysis of selected thermal devices using self-adaptive Jaya algorithm. Energy Convers Manage 2017;140:24–35.
[38] Yu J, Kim C-H, Wadood A, Khurshiad T, Rhee S-B. A novel multi-population based chaotic JAYA algorithm with application in solving economic load dispatch problems. Energies 2018;11:1–26.
[39] Rao RV, Saroj A. Constrained economic optimization of shell-and-tube heat exchangers using elitist-Jaya algorithm. Energy 2017;128:785–800.
[40] Warid W, Hizam H, Mariun N, Abdul-Wahab NI. Optimal power flow using the Jaya algorithm. Energies 2016;9:678.
[41] Warid W, Hizam H, Mariun N, Wahab NIA. A novel quasi-oppositional modified Jaya algorithm for multi-objective optimal power flow solution. Appl Soft Comput 2018;65:360–73.
[42] Wang S-H, Phillips P, Dong Z-C, Zhang Y-D. Intelligent facial emotion recognition based on stationary wavelet entropy and Jaya algorithm. Neurocomputing. 2018;272:668–76.
[43] Kumar N, Hussain I, Singh B, Panigrahi B. Rapid MPPT for uniformly and partial shaded PV system by using JayaDE algorithm in highly fluctuating atmospheric conditions. IEEE Trans Ind Inf 2017;13:2406–16.
[44] Kler D, Sharma P, Banerjee A, Rana KPS, Kumar V. PV cell and module efficient parameters estimation using evaporation rate based water cycle algorithm. Swarm Evol Comput 2017;35:93–110.
[45] Muhsen DH, Ghazali AB, Khatib T, Abed IA. Parameters extraction of double diode photovoltaic module's model based on hybrid evolutionary algorithm. Energy Convers Manage 2015;105:552–61.
[46] Wang XY, Luo DK, Zhao X, Sun Z. Estimates of energy consumption in China using a self-adaptive multi-verse optimizer-based support vector machine with rolling cross-validation. Energy 2018;152:539–48.
[47] Chakri A, Khelif R, Benouaret M, Yang XS. New directional bat algorithm for continuous optimization problems. Expert Syst Appl 2017;69:159–75.
[48] Yu K, Wang X, Wang Z. An improved teaching-learning-based optimization algorithm for numerical and engineering optimization problems. J Intell Manuf 2016;27:831–43.
[49] Easwarakhanthan T, Bottin J, Bouhouch I, Boutrit C. Nonlinear minimization algorithm for determining the solar cell parameters with microcomputers. Int J Solar Energy 1986;4:1–12.
[50] Liang JJ, Qin AK, Suganthan PN, Baskar S. Comprehensive learning particle swarm optimizer for global optimization of multimodal functions. IEEE Trans Evol Comput 2006;10:281–95.
[51] Chen X, Tianfield H, Mei C, Du W, Liu G. Biogeography-based learning particle swarm optimization. Soft Comput 2016:1–23.
[52] Gong WY, Cai Z, Ling CX. DE/BBO: a hybrid differential evolution with biogeography-based optimization for global numerical optimization. Soft Comput 2010;15:645–65.
[53] Chen X, Tianfield H, Du W, Liu G. Biogeography-based optimization with covariance matrix based migration. Appl Soft Comput 2016;45:71–85.
[54] Alcala-Fdez J, Sanchez L, Garcia S, del Jesus MJ, Ventura S, Garrell J, et al. KEEL: a software tool to assess evolutionary algorithms for data mining problems. Soft Comput 2009;13:307–18.
[55] Rajasekar N, Kumar NK, Venugopalan R. Bacterial foraging algorithm based solar PV parameter estimation. Sol Energy 2013;97:255–65.
[56] Merchaoui M, Sakly A, Mimouni MF. Particle swarm optimisation with adaptive mutation strategy for photovoltaic solar cell/module parameter extraction. Energy Convers Manage 2018;175:151–63.
[57] Zekry A, Shaker A, Salem M. Solar cells and arrays: principles, analysis, and design. Advances in renewable energies and power technologies. Elsevier; 2018. p. 3–56.
[58] Olivella-Rosell P, Bullich-Massague E, Aragues-Penalba M, Sumper A, Ottesen SO, Vidal-Clos J-A, et al. Optimization problem for meeting distribution system operator requests in local flexibility markets with distributed energy resources. Appl Energy 2018;210:881–95.
[59] Chen X, Yang H. Integrated energy performance optimization of a passively designed high-rise residential building in different climatic zones of China. Appl Energy 2018;215:145–58.
[60] Yu L, Li YP. A flexible-possibilistic stochastic programming method for planning municipal-scale energy system through introducing renewable energies and electric vehicles. J Clean Prod 2019;207:772–87.